

1.1 CLIMATE AND OCEANIC INDICATORS

Over the past few years, the Council has incorporated climate change into the overall management of the fisheries over which it has jurisdiction. This 2019 Annual SAFE Report includes a now standard chapter on indicators of climate and oceanic conditions in the Western Pacific region. These indicators reflect both global climate variability and change, as well as trends in local oceanographic conditions.

This year, we have reordered the information in this chapter in order to make it more accessible to a broader audience. To this end, we begin with a brief summary of the state of the ocean and climate in 2019. This is followed by a list of all selected indicators. These indicators are then examined through summaries focused on natural climate variability and on anthropogenic climate change. Information on the background of these indicators, their development over time, and ongoing research needs can be found at the end of this chapter.

1.1.1.1 INDICATORS AT A GLANCE

Based on the information provided by the indicators in this chapter, ocean and climate conditions in the Western Pacific region in 2019 were roughly average and long-term climate trends persisted. Modes of interannual climate variability (e.g., ENSO, PDO) were neutral. Hurricane activity was average. The atmospheric concentration of carbon dioxide continued to increase, ocean acidification intensified, and sea surface temperatures continued to rise. Chlorophyll concentrations at the ocean's surface and the median size of phytoplankton continued to decline. Temperatures at 200 – 300 m below the surface were average. Bigeye tuna and swordfish were slightly larger than average, though no long-term trend is evident. Neither the bigeye recruitment index nor the bigeye forecast suggest there will be a pulse of increased recruitment or catch rates in the next few years.

1.1.2 SELECTED INDICATORS

The primary goal for selecting the indicators used in this report is to provide fisheries-related communities, resource managers, and businesses with a climate-related situational awareness. In this context, indicators were selected to:

- Be fisheries relevant and informative.
- Build intuition about current conditions in light of a changing climate;
- Provide historical context; and
- Allow for recognition of patterns and trends.

In this context, this section includes the following climate and oceanic indicators:

- Atmospheric concentration of carbon dioxide (CO₂)
- Oceanic pH at Station ALOHA;
- El Niño – Southern Oscillation (ENSO);
- Pacific Decadal Oscillation (PDO);
- Tropical cyclones;

- Sea surface temperature (SST);
- Ocean temperature at 200 – 300 m depth;
- Ocean color;
- North Pacific Subtropical Front (STF) and Transition Zone Chlorophyll Front (TZCF);
- Estimated Median Phytoplankton Size;
- Fish community size structure;
- Bigeye tuna weight-per-unit-effort;
- Bigeye tuna recruitment index; and
- Bigeye tuna catch rate forecast.

1.1.2.1 NATURAL CLIMATE VARIABILITY SUMMARY

The ocean and climate indicators described in this chapter can be used to understand the effects of natural climate variability. The relationship between these indicators is illustrated in Fig. 1.

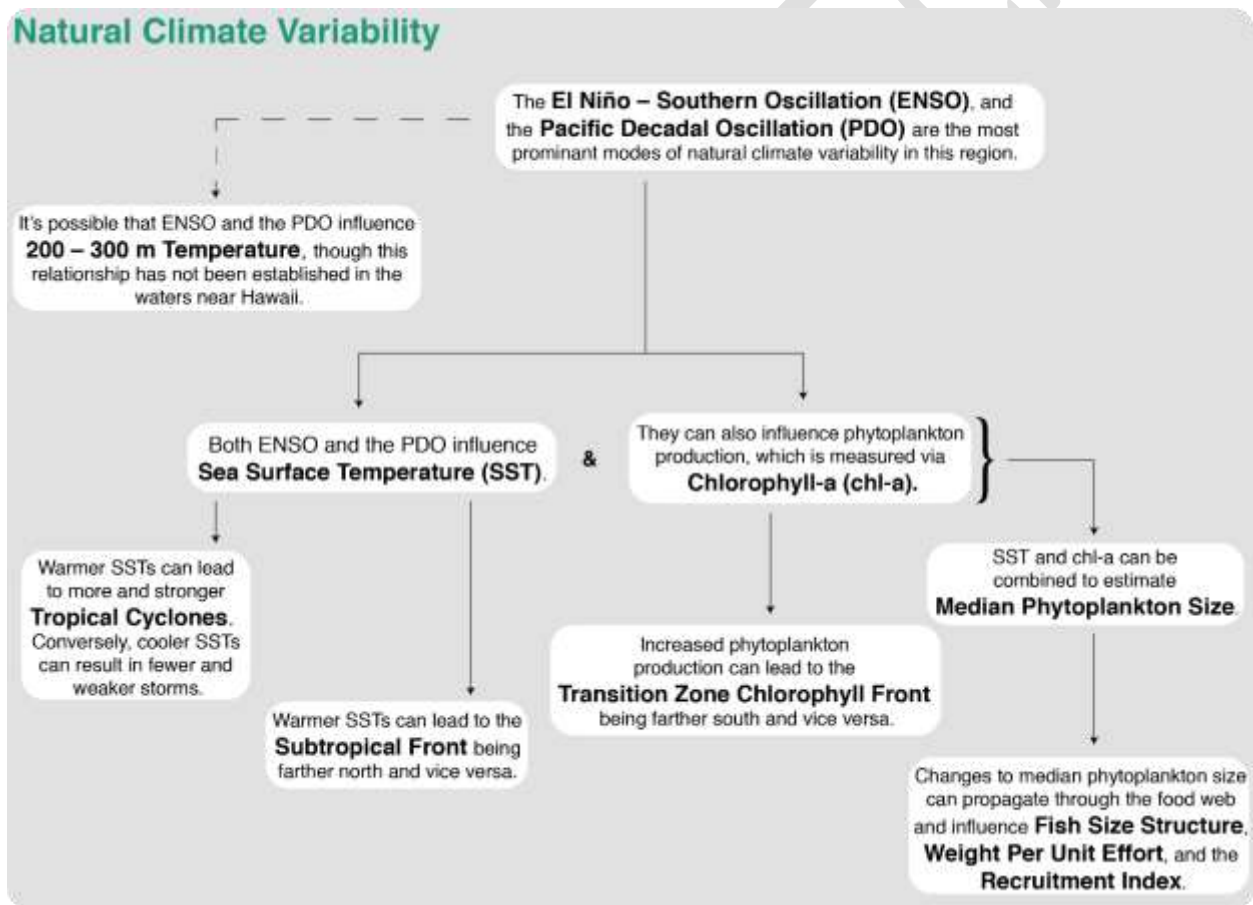


Figure 1 Schematic diagram illustrating the relationships between the ocean and climate indicators from the perspective of natural climate variability.

El Niño – Southern Oscillation (ENSO) and the Pacific Decadal Oscillation (PDO) are the most prominent modes of natural climate variability in this region. ENSO cycles are known to impact

Pacific fisheries including tuna fisheries. The Oceanic Niño Index (ONI) is a measure of ENSO phase that uses ocean temperature, which has the most direct effect on these fisheries. In 2019, ENSO phase transitioned from a weak El Niño to neutral conditions. Like ENSO, the PDO reflects changes between periods of persistently warm or persistently cool temperatures, except over periods of 20 to 30 years (versus six to 18 months for ENSO events). The climatic fingerprints of the PDO are most visible in the Northeastern Pacific, but secondary signatures exist in the tropics. The PDO hovered around zero in 2019. The year was nearly evenly split between values that were slightly negative (seven months) and values that were slightly positive (5 months).

Both ENSO and the PDO influence sea surface temperature (SST), which is one of the most directly observable existing measures for tracking ocean temperature. Natural variability in SST impacts the marine ecosystem and pelagic fisheries. For example, warmer SSTs can lead to the subtropical front being farther north and vice versa, which in turn affects the distance fishers may need to travel to reach longline fishing grounds. Changes in SST can also influence the number, location, strength, and seasonal timing of tropical cyclones. In 2019, SST was above the long-term average across Hawaii's longline fishing grounds. During the first quarter of the year, when the swordfish fishery is most active, the subtropical front that roughly aligns with their fishing ground was close to its average latitude between 155 – 130°W and slightly north of average east and west of this area. The number of named storms and hurricanes/typhoons/cyclones, including major storms, was about average in all basins. The Accumulated Cyclone Energy (ACE) index, a measure of the intensity and duration of storms over the entire season, was below average in all basins.

ENSO and the PDO can also influence phytoplankton production, which is measured via chlorophyll-a (chl-a). Phytoplankton are the foundational food source for the species targeted by the region's longline fishery. Changes in phytoplankton abundance have the potential to impact fish abundance, size, and catch. Increased phytoplankton production can lead to the transition zone chlorophyll front being farther south and vice versa, and changes in the location of this front particularly impact Hawaii's swordfish fishery. In 2019, surface chlorophyll was close to or just below average across much of the longline fishing grounds. The Transition Zone Chlorophyll Front (TZCF), which is targeted by the swordfish fishery, was north of average across nearly the entire fishing grounds in the first quarter of the year. In a few places, it was several degrees north of average.

SST and chl-a can be combined to estimate median phytoplankton size. In 2019, average median phytoplankton size across the longline fishing grounds was below average. Changes to median phytoplankton can propagate through the food web and influence fish size structure, weight per unit effort, and the bigeye tuna recruitment index. Furthermore, the recruitment index can be combined median phytoplankton size to forecast bigeye tuna catch rates four years in advance. Overall, bigeye tuna and swordfish were slightly larger than average in 2019. Weight-per-unit-effort was below average in 2019. The recruitment index was similar to the previous few years and does not suggest an upcoming recruitment pulse. Similarly, the bigeye catch rate forecast suggest only a very moderate increase in catch rates over the next four years.

It's possible that natural climate variability influences temperatures at 200 – 300 m below the surface where the bigeye fishery sets their hooks. However, this relationship has yet to be established. At 200 – 300 meters depth, waters around Hawaii and in the southwestern portion of the bigeye tuna fishing grounds were up to 1 °C cooler than average in 2019. In the northeastern portion of the fishing grounds and between about 30 – 40°N, waters were slightly warmer than average.

Understanding the effects of natural climate variability, like ENSO and the PDO, on the ocean, marine ecosystems, and the fishery is an active area of research.

1.1.2.2 ANTHROPOGENIC CLIMATE CHANGE SUMMARY

The ocean and climate indicators described in this chapter can be used to understand the effects of natural climate variability. The relationship between these indicators is illustrated in Fig. 2.

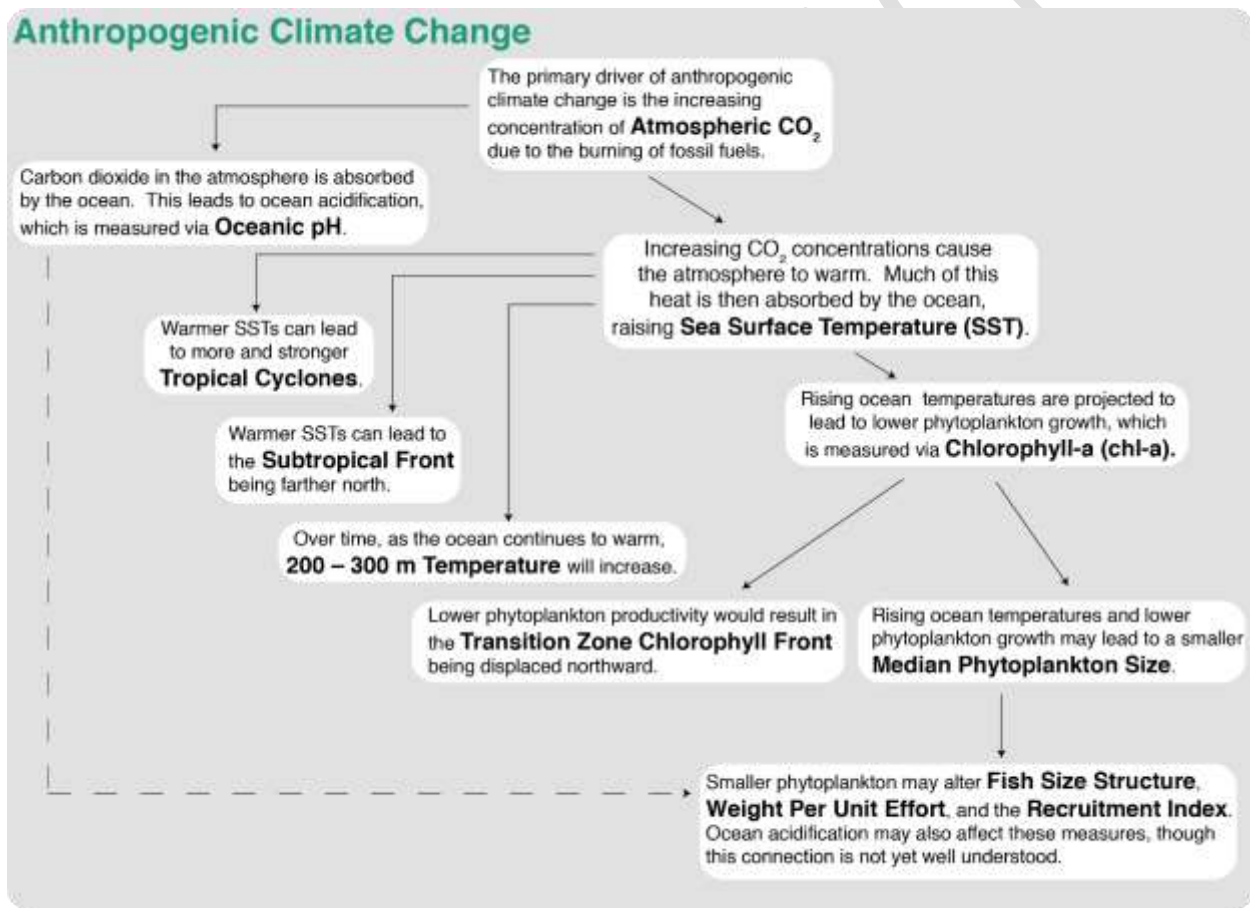


Figure 2 Schematic diagram illustrating the relationships between the ocean and climate indicators from the perspective of anthropogenic climate change.

The primary driver of anthropogenic (human-caused) climate change is the increasing concentration of atmospheric carbon dioxide, CO₂, due to the burning of fossil fuels. Therefore, atmospheric CO₂ serves as a measure of what human activity has already done to affect the

climate system through greenhouse gas emissions. The concentration of atmospheric CO₂, and, in turn, its warming influence, is increasing at a faster rate each year. In 2019, the annual mean concentration of CO₂ was 411 ppm. In 1959, the first year of the time series, it was 316 ppm. The annual mean passed 350 ppm in 1988, and 400 ppm in 2015.

Carbon dioxide in the atmosphere is absorbed by the ocean. This leads to ocean acidification, which is measured via pH. Therefore, oceanic pH is a measure of how greenhouse gas emissions have already impacted the ocean. Increasing ocean acidification limits the ability of marine organisms to build shells and other hard structures. Prey for commercially-valuable fish are already being negatively affected by increasing ocean acidification. In 2018, the most recent year for which data are available, the average pH at Station ALOHA was 8.07. The ocean is now roughly 9.7% more acidic than it was nearly 30 years ago at the start of this time series. Over this time, pH has declined by 0.0401 at a constant rate.

Increasing carbon dioxide concentrations cause the atmosphere to warm. Much of this heat is then absorbed by the ocean, raising sea surface temperature (SST). Over the past 35 years, SST in the Hawaii longline region has increased at a rate of 0.02 °C yr⁻¹. In 2019, annual mean SST was 21.1 °C. Monthly SST values in 2019 ranged from 18.2 – 24.7 °C, exceeding the previous maximum of 24.6 °C.

Rising sea surface temperatures may affect the number, strength, duration, and seasonal timing of tropical cyclones. The Accumulated Cyclone Energy index, or ACE Index, accounts for both the strength and duration of storms. There has been no significant trend in the number or strength (measured via Accumulated Cyclone Energy, or ACE, index) of tropical cyclones from 1980 through 2019.

Over time, rising sea surface temperatures will warm deeper ocean waters. Changes in ocean temperature will affect tuna, and in turn, potentially their catchability. For example, fish may move to deeper waters or their habitat could be compressed geographically or vertically. Temperatures at 200 – 300 meters below the ocean's surface reflect those at the mid-range of depths targeted by the deep-set bigeye tuna fishery. Bigeye tuna have preferred thermal habitat, generally staying within waters between 8 – 14 °C while they are at depth. Over the past 39 years, 200 – 300-meter temperatures have ranged from 10.87 – 11.58 °. There has been no meaningful trend in these temperatures over this period of record. In 2019, 200 – 300 m temperatures ranged from 10.96 – 11.22 °C with an average value of 11.09 °C. Temperatures in 2019 were 0.02 – 0.2 °C below average, though within the range of previously observed temperatures.

Rising ocean temperatures are projected to lead to lower phytoplankton growth, which is measured via chlorophyll-a (chl-a). Over the past 22 years, monthly chlorophyll-a has declined by 0.015 mg chl m⁻³ across the longline fishing grounds. Combined, rising ocean temperatures and lower phytoplankton growth may lead to smaller median phytoplankton sizes. Median phytoplankton size over the longline fishing grounds has steadily declined by 0.13µm over the period of record. Smaller phytoplankton may alter fish size structure, weight per unit effort, and the bigeye tuna recruitment index. Median phytoplankton size can be combined with the bigeye

recruitment index to forecast catch rates. Over the period of record, there is no trend in the median size of fish caught by Hawaii’s longline fishery or the recruitment index.

Understanding the effects of anthropogenic climate change on the ocean, marine ecosystems, and the fishery is an active area of research.

1.1.2.3 ATMOSPHERIC CONCENTRATION OF CARBON DIOXIDE (CO₂) AT MAUNA LOA

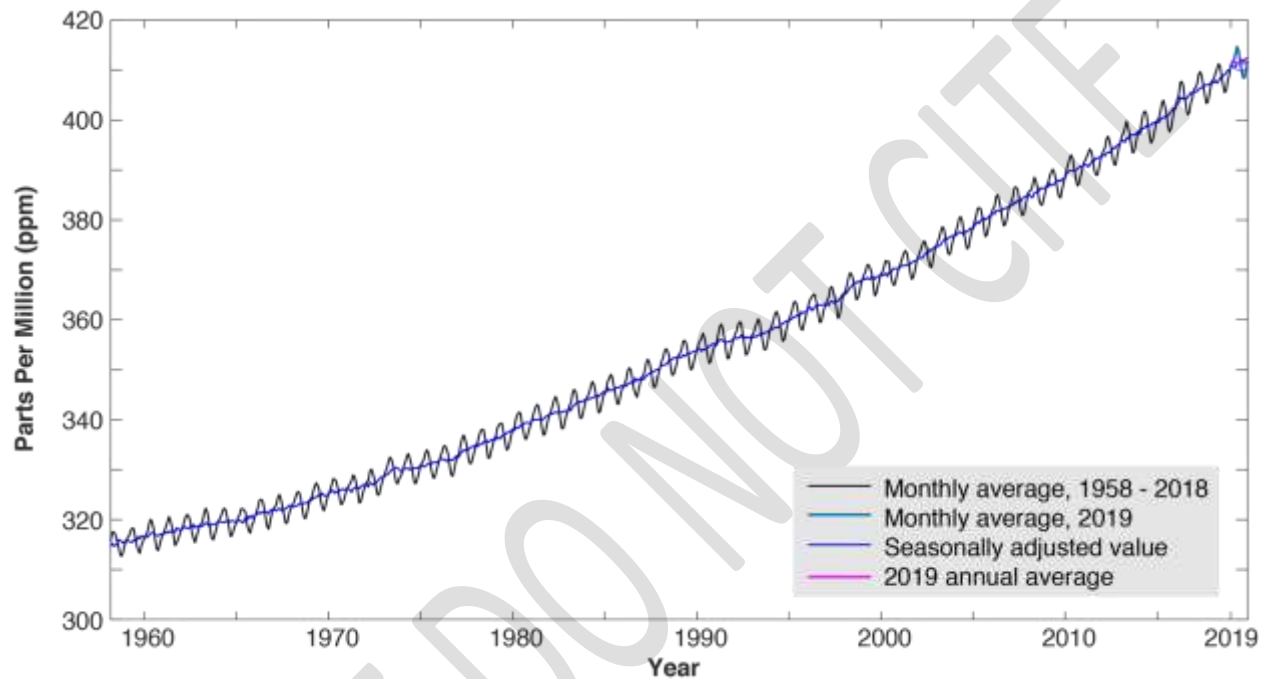


Figure 3 The concentration of atmospheric carbon dioxide at Mauna Loa Observatory on the island of Hawai‘i.

Rationale: Atmospheric carbon dioxide is a measure of what human activity has already done to affect the climate system through greenhouse gas emissions. It provides quantitative information in a simplified, standardized format that decision makers can easily understand. This indicator demonstrates that the concentration (and, in turn, warming influence) of greenhouse gases in the atmosphere has increased substantially over the last several decades.

Status: Atmospheric CO₂ is increasing exponentially. This means that atmospheric CO₂ is increasing at a faster rate each year. In 2019, the annual mean concentration of CO₂ was 411 ppm. In 1959, the first year of the time series, it was 316 ppm. The annual mean passed 350 ppm in 1988, and 400 ppm in 2015.

Description: Monthly mean atmospheric carbon dioxide (CO₂) at Mauna Loa Observatory, Hawai‘i in parts per million (ppm) from March 1958 to present. The observed increase in monthly average carbon dioxide concentration is primarily due to CO₂ emissions from fossil fuel burning. Carbon dioxide remains in the atmosphere for a very long time, and emissions from any

location mix throughout the atmosphere in approximately one year. The annual variations at Mauna Loa, Hawai`i are due to the seasonal imbalance between the photosynthesis and respiration of terrestrial plants. During the summer growing season, photosynthesis exceeds respiration, and CO₂ is removed from the atmosphere. In the winter (outside the growing season), respiration exceeds photosynthesis, and CO₂ is returned to the atmosphere. The seasonal cycle is strongest in the northern hemisphere because of its larger land mass.

Timeframe: Annual, monthly.

Region/Location: Mauna Loa, Hawai`i, but representative of global atmospheric carbon dioxide concentration.

Measurement Platform: *In-situ* station.

Sourced from: Keeling et al. (1976), Thoning et al. (1989), and NOAA (2020b).

1.1.2.4 OCEANIC PH

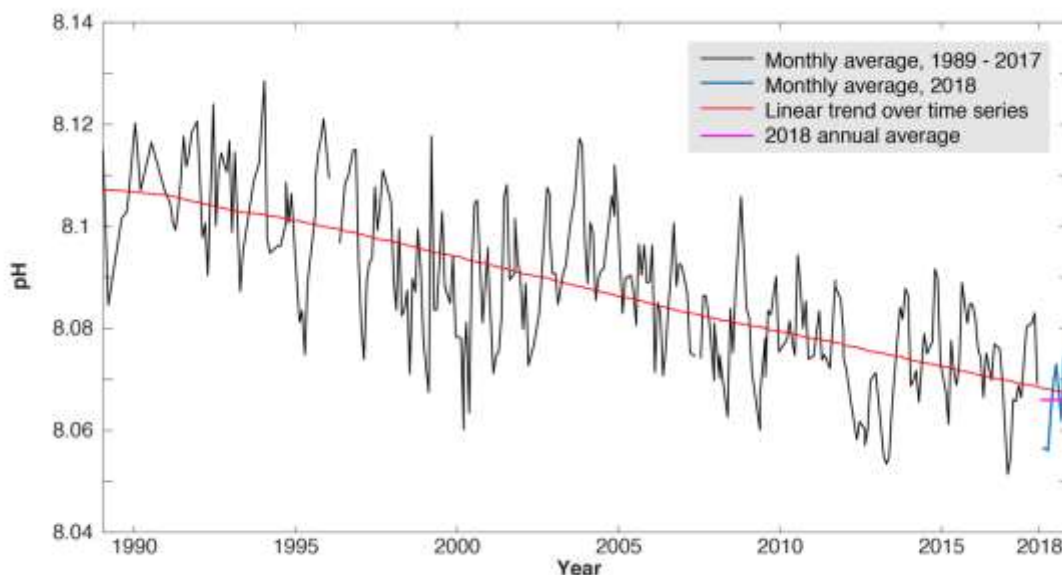


Figure 4 Time series and long-term trend of oceanic pH measured at Station ALOHA.

Rationale: Oceanic pH is a measure of how greenhouse gas emissions have already impacted the ocean. This indicator demonstrates that oceanic pH has decreased significantly over the past several decades (i.e. the ocean has become more acidic). Increasing ocean acidification limits the ability of marine organisms to build shells and other calcareous structures. Recent research has shown that pelagic organisms such as pteropods and other prey for commercially-valuable fish species are already being negatively impacted by increasing acidification (Feely *et al.*, 2016). The full impact of ocean acidification on the pelagic food web is an area of active research (Fabry *et al.*, 2008).

Status: The ocean is roughly 9.7% more acidic than it was nearly 30 years ago at the start of this time series. Over this time, pH has declined by 0.0401 at a constant rate. In 2018, the most recent year for which data are available, the average pH was 8.07. Additionally, small variations seen over the course of the year are outside the range seen in the first year of the time series for the second year in a row. The highest pH value reported for the most recent year (8.0743, down from a high of 8.0830 in 2017) is lower than the lowest pH value reported in the first year of the time series (8.0845).

Description: Trends in surface (5 m) pH at Station ALOHA, north of Oahu (22.75°N, 158°W), collected by the Hawai'i Ocean Time Series (HOT) from October 1988 to 2016 (2017 data are not yet available). Oceanic pH is a measure of ocean acidity, which increases as the ocean absorbs carbon dioxide from the atmosphere. Lower pH values represent greater acidity. Oceanic pH is calculated from total alkalinity (TA) and dissolved inorganic carbon (DIC). Total alkalinity represents the ocean's capacity to resist acidification as it absorbs CO₂ and the amount of CO₂ absorbed is captured through measurements of DIC. The multi-decadal time series at Station ALOHA represents the best available documentation of the significant downward trend in oceanic pH since the time series began in 1988. Oceanic pH varies over both time and space, though the conditions at Station ALOHA are considered broadly representative of those across the Western and Central Pacific's pelagic fishing grounds.

Timeframe: Monthly.

Region/Location: Station ALOHA: 22.75°N, 158°W.

Measurement Platform: *In-situ* station.

Sourced from: Fabry et al. (2008), Feely et al. (2016), and the Hawaii Ocean Time Series as described in Karl et al. (1996) and on its website (HOT, 2020).

1.1.2.5 EL NIÑO – SOUTHERN OSCILLATION (ENSO)

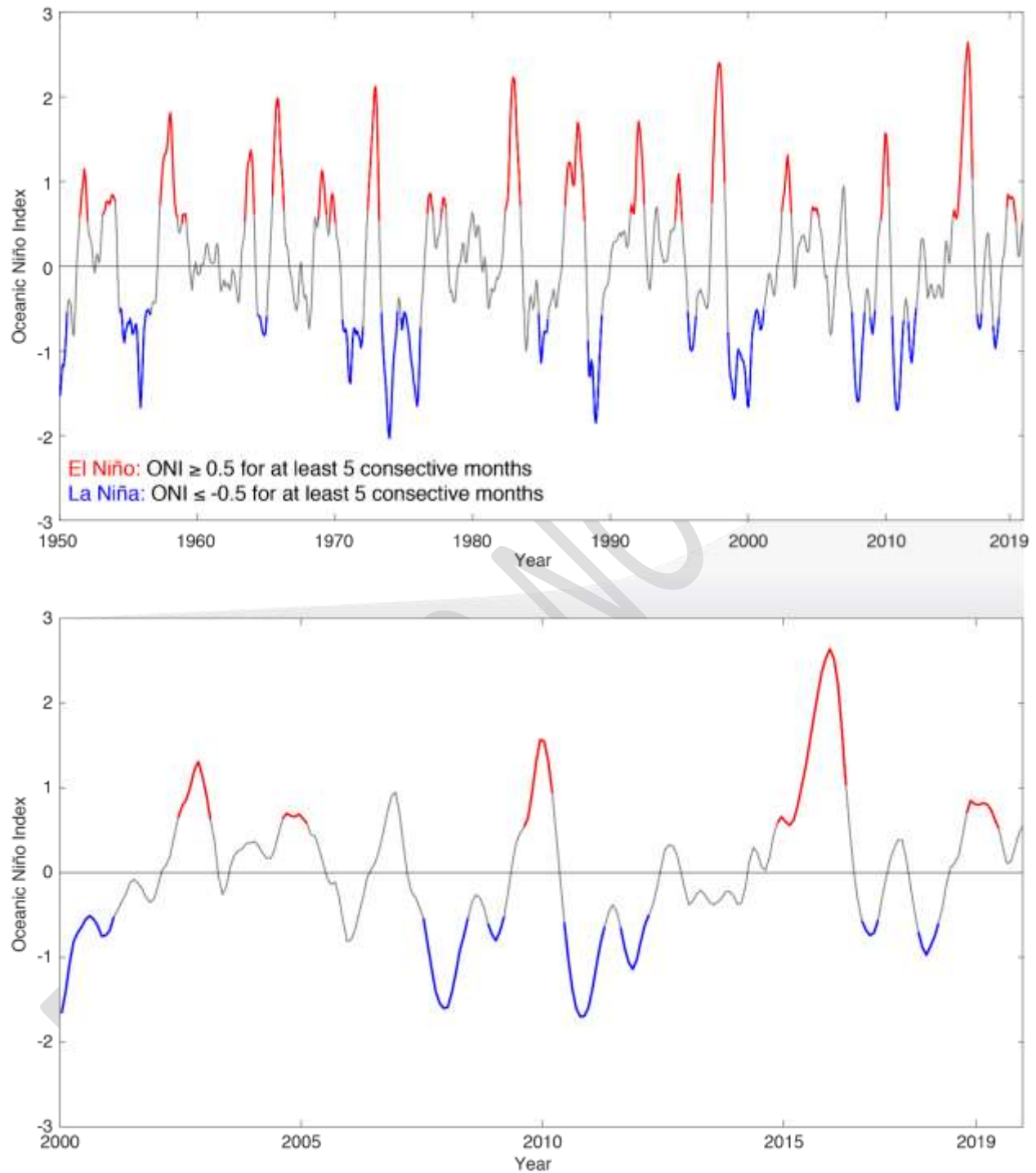


Figure 5 Oceanic Niño Index from 1950-2018 (top) and 2000–2018 (bottom) with El Niño periods in red and La Niña periods in blue.

Rationale: The El Niño – Southern Oscillation (ENSO) cycle is known to have impacts on Pacific fisheries including tuna fisheries. The ONI focuses on ocean temperature, which has the most direct effect on these fisheries.

Status: In 2019, the ONI transitioned from a weak El Niño to neutral conditions.

Description: The three-month running mean of satellite remotely-sensed sea surface temperature (SST) anomalies in the Niño 3.4 region (5°S – 5°N, 120° – 170°W). The Oceanic Niño Index (ONI) is a measure of the El Niño – Southern Oscillation (ENSO) phase. Warm and cool phases, termed El Niño and La Niña respectively, are based in part on an ONI threshold of ± 0.5 °C being met for a minimum of five consecutive overlapping seasons. Additional atmospheric indices are needed to confirm an El Niño or La Niña event, as the ENSO is a coupled ocean-atmosphere phenomenon. The atmospheric half of ENSO is measured using the Southern Oscillation Index.

Timeframe: Every three months.

Region/Location: Niño 3.4 region, 5°S – 5°N, 120° – 170°W.

Measurement Platform: *In-situ* station, satellite, model.

Sourced from NOAA CPC (2020).

1.1.2.6 PACIFIC DECADAL OSCILLATION (PDO)

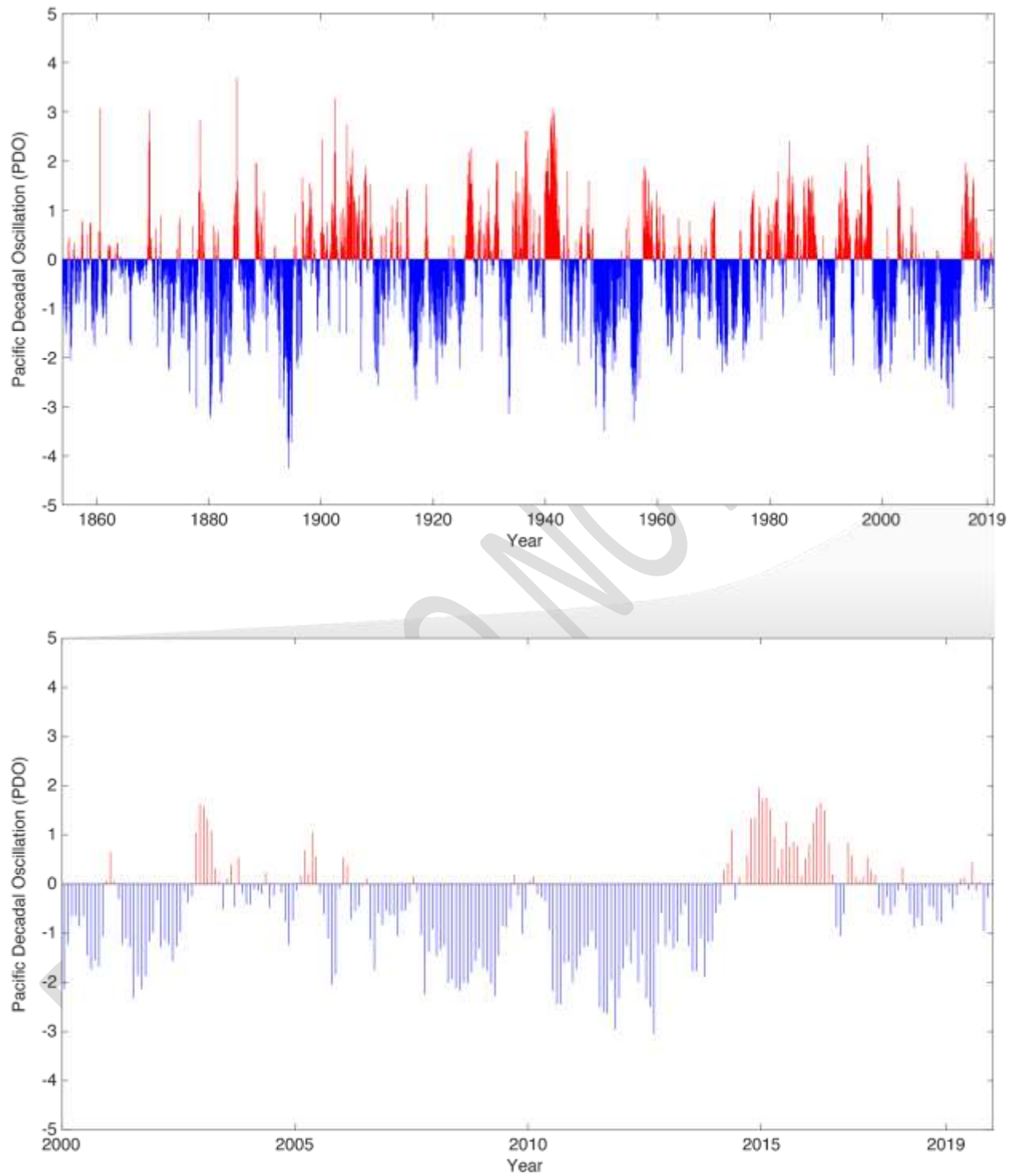


Figure 6 Pacific Decadal Oscillation from 1950–2018 (top) and 2000–2018 (bottom) with positive warm periods in red and negative cool periods in blue.

Rationale: The Pacific Decadal Oscillation (PDO) was initially named by fisheries scientist Steven Hare in 1996 while researching connections between Alaska salmon production cycles and Pacific climate. Like ENSO, the PDO reflects changes between periods of persistently warm or persistently cool ocean temperatures, but over a period of 20 to 30 years (versus six to 18 months for ENSO events). The climatic finger prints of the PDO are most visible in the Northeastern Pacific, but secondary signatures exist in the tropics.

Status: The PDO hovered around zero in 2019. The year was nearly evenly split between values that were slightly negative (seven months) and values that were slightly positive (5 months).

Description: The PDO is often described as a long-lived El Niño-like pattern of Pacific climate variability. As seen with the better-known ENSO, extremes in the PDO pattern are marked by widespread variations in the Pacific Basin and the North American climate. In parallel with the ENSO phenomenon, the extreme cases of the PDO have been classified as either warm or cool, as defined by ocean temperature anomalies in the northeast and tropical Pacific Ocean. When SST is below average in the interior North Pacific and warm along the North American coast, and when sea level pressures are below average in the North Pacific, the PDO has a positive value. When the climate patterns are reversed, with warm SST anomalies in the interior and cool SST anomalies along the North American coast, or above average sea level pressures over the North Pacific, the PDO has a negative value. (<https://www.ncdc.noaa.gov/teleconnections/pdo/>).

Timeframe: Annual, monthly.

Region/Location: Pacific Basin north of 20°N.

Measurement Platform: *In-situ* station, satellite, model.

Sourced from: NOAA ESRL (2020a)

1.1.2.7 TROPICAL CYCLONES

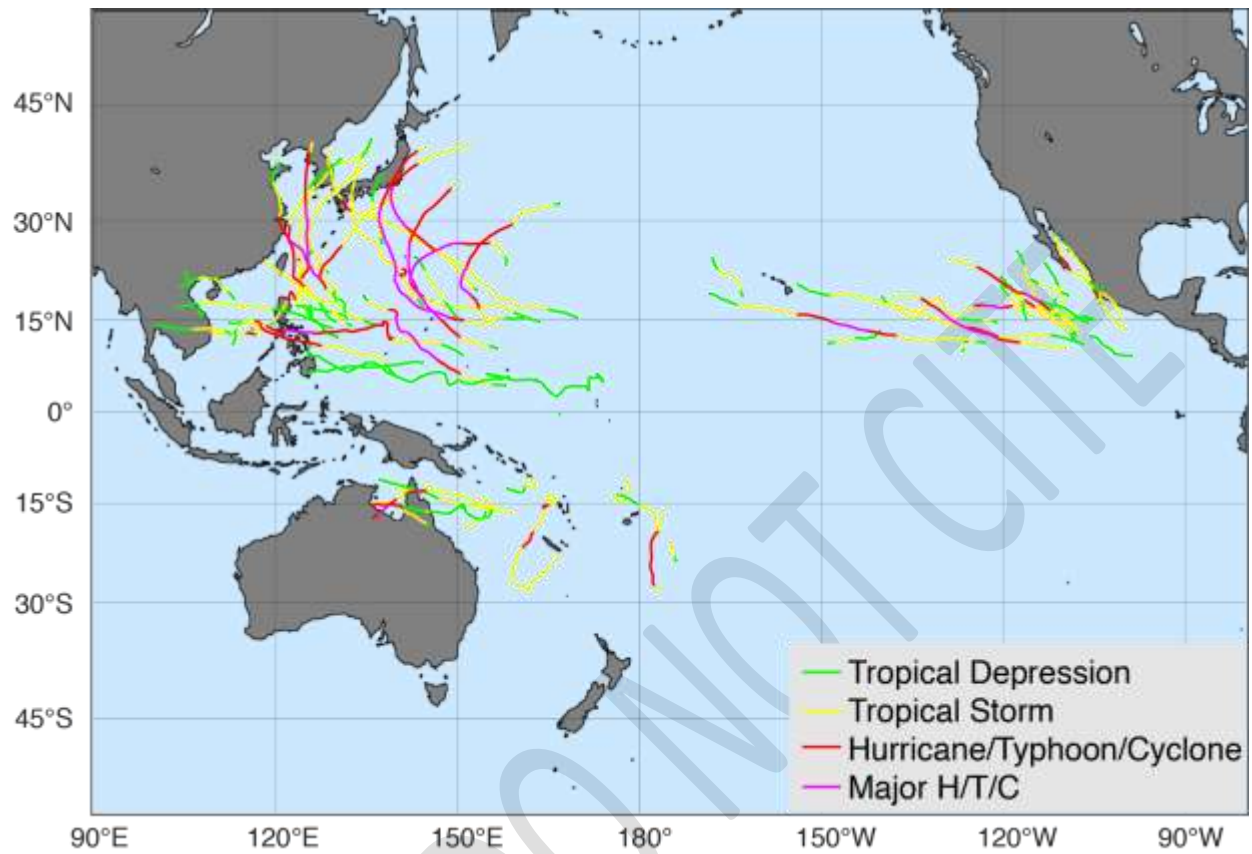


Figure 7 2019 Pacific basin tropical cyclone tracks.

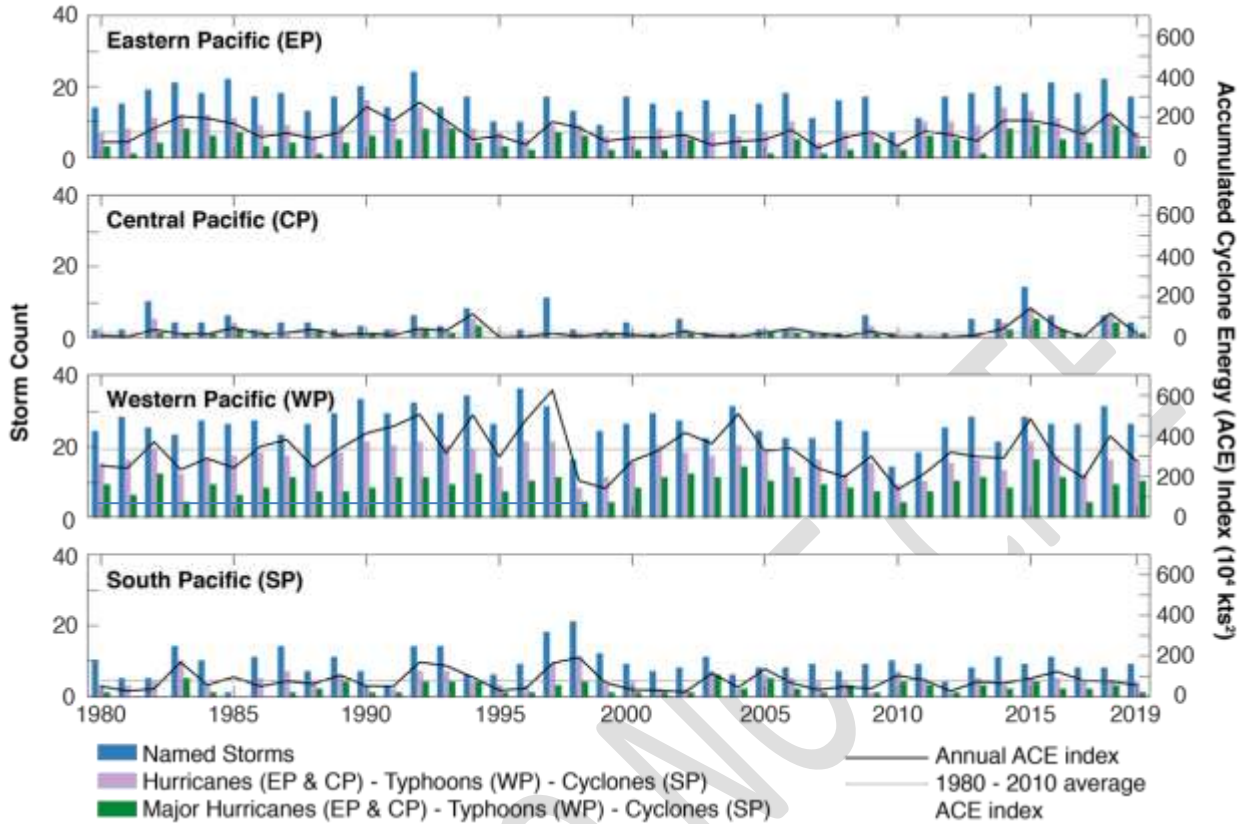


Figure 8 Storm counts (bars) and Accumulated Cyclone Energy (ACE) index values (lines) in each region of the Pacific. Both annual ACE index (black lines) and 1981 – 2010 average ACE index (grey lines) are shown.

Rationale: The effects of tropical cyclones are numerous and well known. At sea, storms disrupt and endanger shipping traffic as well as fishing effort and safety. The Hawai`i longline fishery, for example, has had serious problems with vessels dodging storms at sea, delayed departures, and inability to make it safely back to Honolulu because of bad weather. When cyclones encounter land, their intense rains and high winds can cause severe property damage, loss of life, soil erosion, and flooding. Associated storm surge, the large volume of ocean water pushed toward shore by cyclones’ strong winds, can cause severe flooding and destruction.

Status:

Eastern North Pacific. Overall, the 2019 eastern Pacific hurricane season featured near average activity. There were 17 named storms, of which seven became hurricanes and three became major hurricanes - category 3 or higher on the Saffir-Simpson Hurricane Wind Scale. This compares to the long-term averages of fifteen named storms, eight hurricanes, and four major hurricanes. There were also two tropical depressions that did not reach tropical storm strength. In terms of Accumulated Cyclone Energy (ACE), which measures the strength and duration of tropical storms and hurricanes, activity in the basin in 2019 was a little below the long-term mean. Summary inserted from <https://www.nhc.noaa.gov/text/MIATWSEP.shtml>.

Central North Pacific. Tropical cyclone activity in the central Pacific in 2019 was average. There were four named storms, of which one became a hurricane and one became a major hurricane. The ACE index was slightly below the 1981 – 2010 average of roughly 20×10^4 knots²).

Western North Pacific. Tropical cyclone activity was roughly average in the western Pacific in 2019. There were 26 named storms. Sixteen of these storms developed into typhoons, and ten of these typhoons were major. The ACE Index was below the 1981 – 2010 average. Of note was Super typhoon Hagibis. Hagibis was just the third category 5 tropical cyclone globally in 2019 (Super Typhoon Wutip and Hurricane Dorian were the others). Hagibis weakened to a category 2 storm before making landfall in Japan, but was still one of the most damaging typhoons in history. The remnants of Hagibis transitioned to an extratropical cyclone that affected the Aleutian Islands and significantly altered the weather patterns over the North America in the subsequent days. Summary inserted from <https://www.ncdc.noaa.gov/sotc/tropical-cyclones/201910>.

South Pacific. Tropical cyclone activity was average in the south Pacific region in 2019. There were nine named storms, four of which developed into cyclones and one of which was a major cyclone. The ACE Index were below average in 2018.

Description: This indicator uses historical data from the NOAA National Climate Data Center (NCDC) International Best Track Archive for Climate Stewardship to track the number of tropical cyclones in the western, central, eastern, and southern Pacific basins. This indicator also monitors the Accumulated Cyclone Energy (ACE) Index and the Power Dissipation Index which are two ways of monitoring the frequency, strength, and duration of tropical cyclones based on wind speed measurements.

The annual frequency of storms passing through each basin is tracked and a bar plots shows the representative breakdown of Saffir-Simpson hurricane categories.

Every cyclone has an ACE Index value, which is a number based on the maximum wind speed measured at six-hourly intervals over the entire time that the cyclone is classified as at least a tropical storm (wind speed of at least 34 knots; 39 mph). Therefore, a storm's ACE Index value accounts for both strength and duration. This plot shows the historical ACE values for each hurricane/typhoon season and has a horizontal line representing the average annual ACE value.

Timeframe: Annual.

Region/Location:

Eastern North Pacific: east of 140° W, north of the equator.

Central North Pacific: 180° - 140° W, north of the equator.

Western North Pacific: west of 180°, north of the equator.

South Pacific: south of the equator.

Measurement Platform: Satellite.

Sourced from: Knapp et al. (2010), Knapp et al. (2018)

DRAFT DO NOT CITE

1.1.2.8 SEA SURFACE TEMPERATURE (SST)

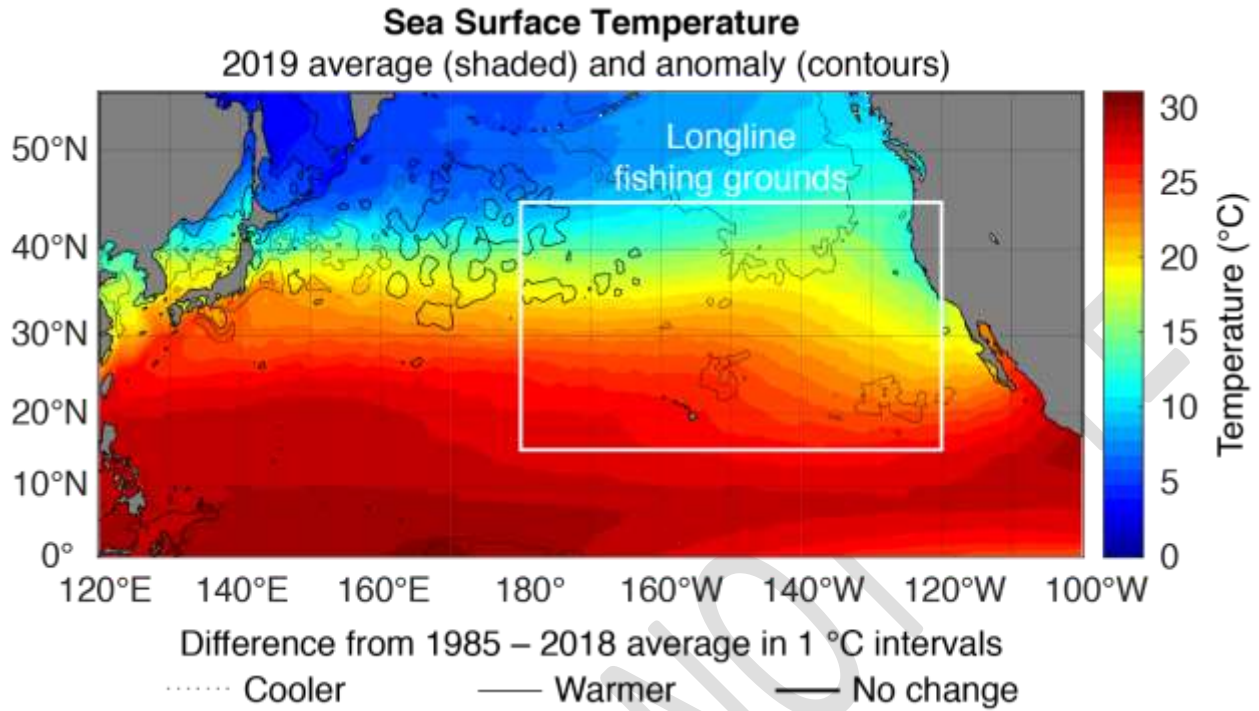


Figure 9 Average 2019 sea surface temperature (shaded) and the difference from the 1985 – 2018 average (contoured). The white rectangle identifies the area targeted by Hawaii’s longline fisheries. SST is averaged over this area for the time series shown in Fig. 10 and 11.

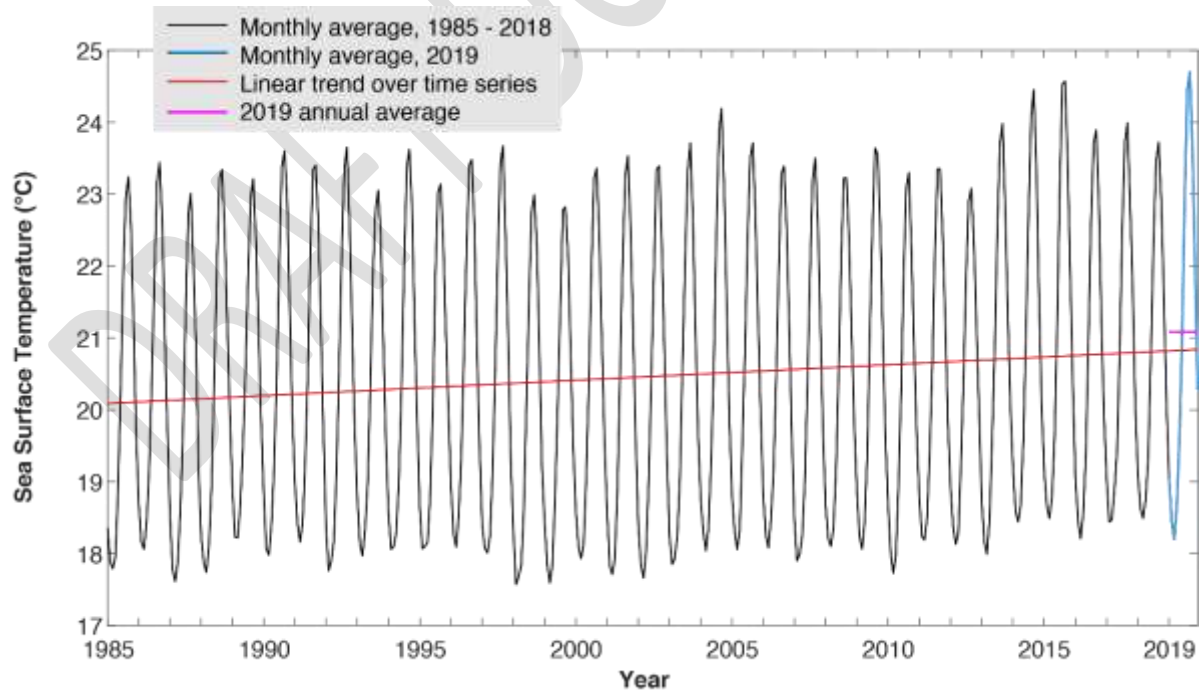


Figure 10 Time series of monthly average sea surface temperature over the longline fishing grounds outlined in Fig. 9.

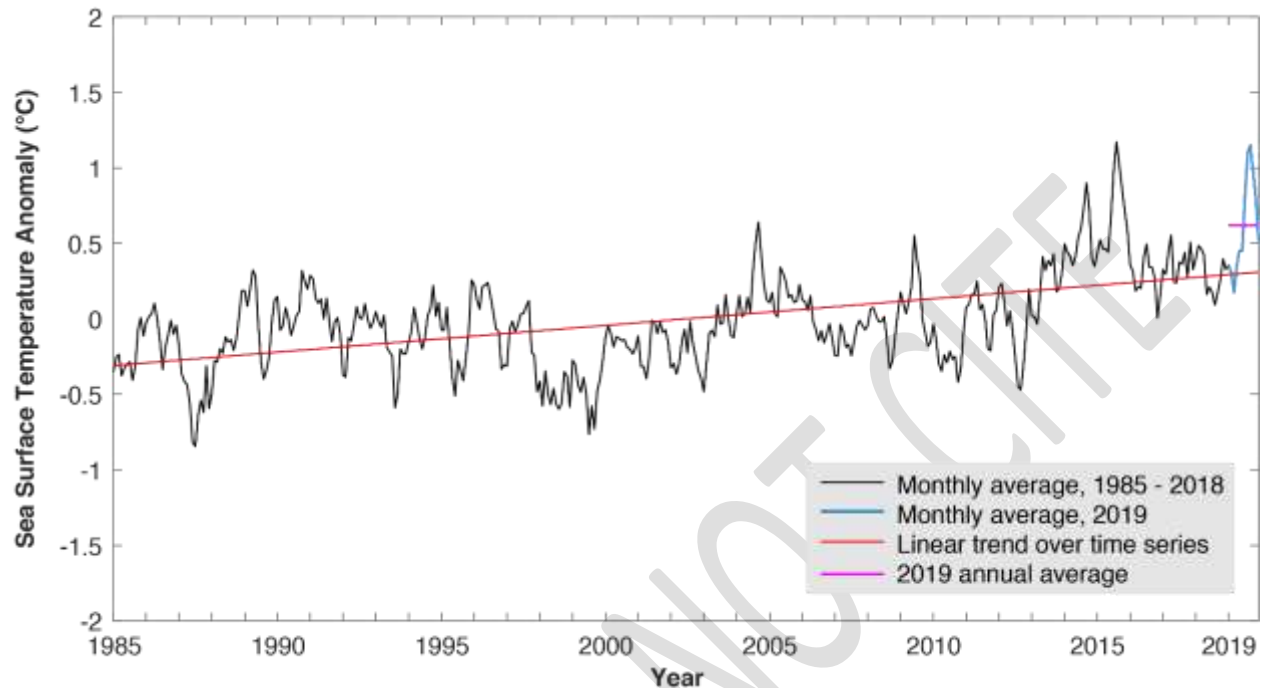


Figure 11 Time series of monthly average sea surface temperature anomaly over the longline fishing grounds outlined in Fig. 9.

Rationale: Sea surface temperature is one of the most directly observable existing measures for tracking increasing ocean temperatures. SST varies in response to natural climate cycles such as the El Niño – Southern Oscillation (ENSO) and is projected to rise as a result of anthropogenic climate change. Both short-term variability and long-term trends in SST impact the marine ecosystem. Understanding the mechanisms through which organisms are impacted and the time scales of these impacts is an area of active research.

Status: Annual mean SST was 21.1 °C in 2019. Over the period of record, annual SST has increased at a rate of 0.02 °C yr⁻¹. Monthly SST values in 2019 ranged from 18.2 – 24.7 °C, exceeding the previous maximum of 24.6 °C. Overall, SST was above the long-term average across the Hawaii longline region in 2019.

Description: Satellite remotely-sensed monthly sea surface temperature (SST) is averaged across the Hawai`i-based longline fishing grounds (15° – 45°N, 180° – 120°W). A time series of monthly mean SST averaged over the Hawai`i longline region is presented. Additionally, spatial climatologies and anomalies are shown. CoralTemp data are used to calculate this indicator.

Timeframe: Monthly.

Region/Location: Hawai`i longline region: 15° – 45°N, 180° – 120°W.

Measurement Platform: Satellite.

Sourced from: NOAA OceanWatch (2020).

1.1.2.9 TEMPERATURE AT 300 M DEPTH

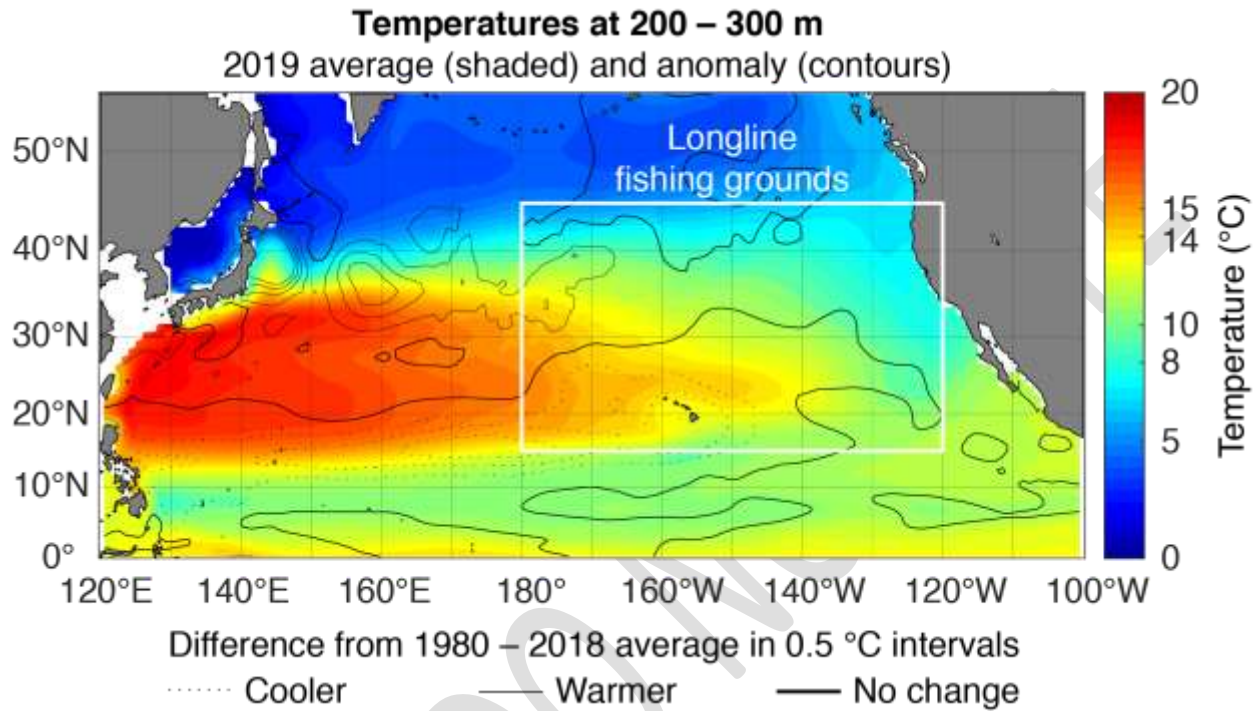


Figure 12 Average temperatures at 200 – 300 m depth in 2019 (shaded) and the difference from the 1980 – 2018 average (contoured). The white rectangle identifies the area targeted by Hawaii’s longline fisheries. Temperatures is averaged over this area for the time series shown in Fig. 13.

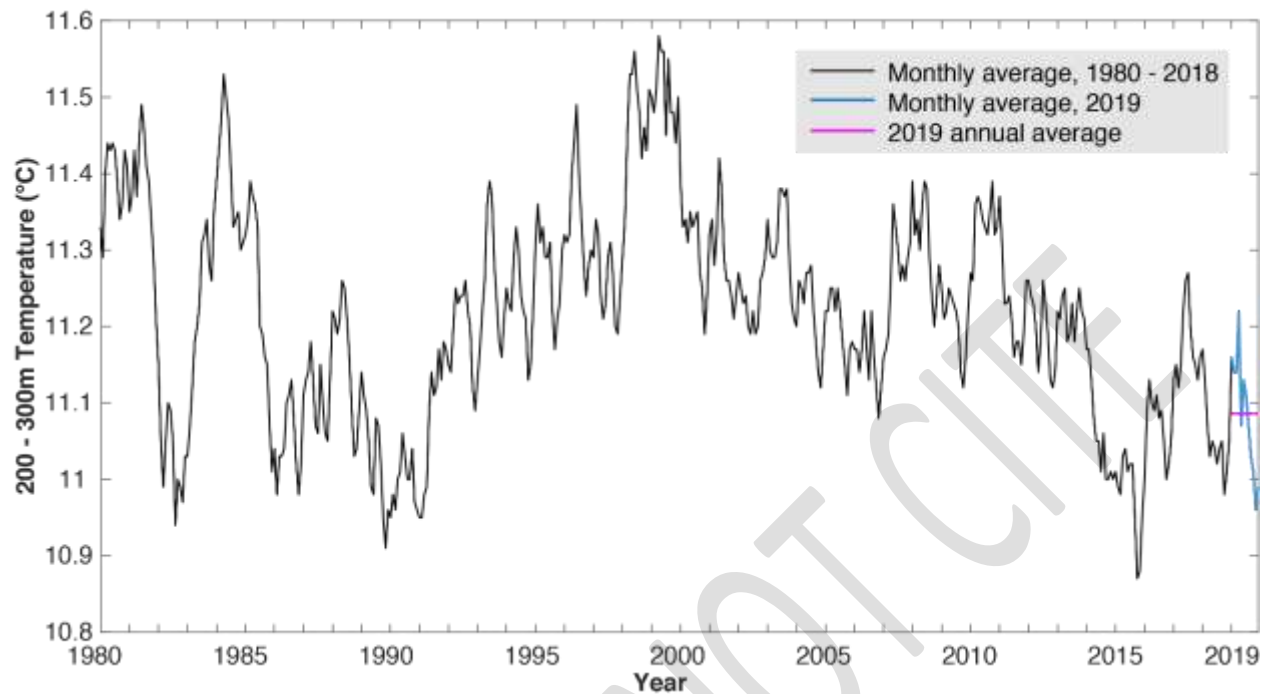


Figure 13 Time series of monthly 200 – 300 m temperatures over the longline fishing grounds outlined in Fig. 12.

Rationale: The temperature at 200 – 300 m reflects the temperature in the mid-range of depths targeted by the deep-set bigeye tuna fishery. Bigeye have preferred thermal habitat, generally staying within temperatures ranging from 8 – 14 °C while they are at depth (Howell et al., 2010). Changes in ocean temperature at depth will impact tuna, and in turn, potentially impact their catchability. Understanding the drivers of sub-surface temperature trends and their ecosystem impacts is an area of active research.

Status: In 2019, 200 – 300 m temperatures ranged from 10.96 – 11.22 °C with an average value of 11.09 °C. These temperatures are within the range of temperatures experienced over the past several decades (10.87 – 11.58 °C) and are within the bounds of bigeye tuna’s preferred deep daytime thermal habitat (8 – 14 °C). Over the period of record (1980 – 2019), 200 – 300 m temperatures have declined by 0.08 °C. The spatial pattern of temperature anomalies was mixed with cooler than average temperatures at depth in the southern portion of the fishing grounds and around the main Hawaiian Islands, and warmer than average temperatures in the mid-latitudes and the northeastern region of the fishing grounds.

Description: Ocean temperature at 200 – 300 m depth is averaged across the Hawai`i-based longline fishing grounds (15° – 45°N, 180° – 120°W). Global Ocean Data Assimilation System (GODAS) data are used. GODAS incorporates global ocean data from moorings, expendable bathythermographs (XBTs), and Argo floats.

Timeframe: Annual, monthly.

Region/Location: Hawai`i longline region: 15° – 45°N, 180° – 120°W.

Measurement Platform: *In-situ* sensors, model.

Sourced from: NOAA ESRL (2020c).

DRAFT DO NOT CITE

1.1.2.10 OCEAN COLOR

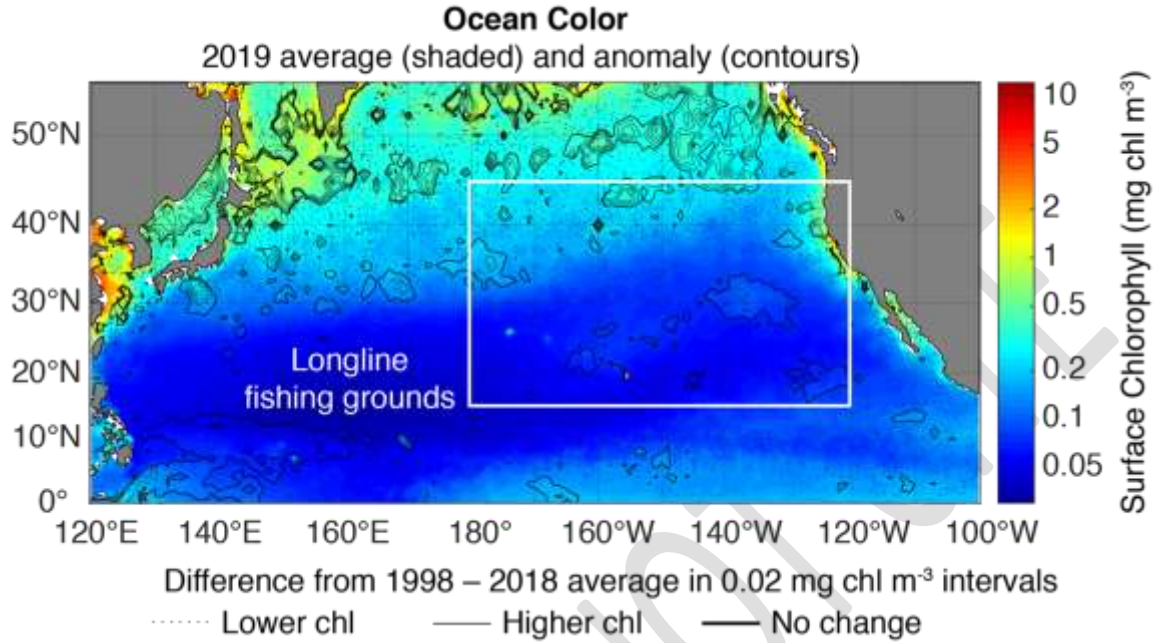


Figure 14 Average ocean color in 2019 (shaded) and the difference from the 1998 – 2018 average (contoured). The white rectangle identifies the area targeted by Hawaii’s longline fisheries. Ocean color is averaged over this area for the time series shown in Figs. 15 and 16.

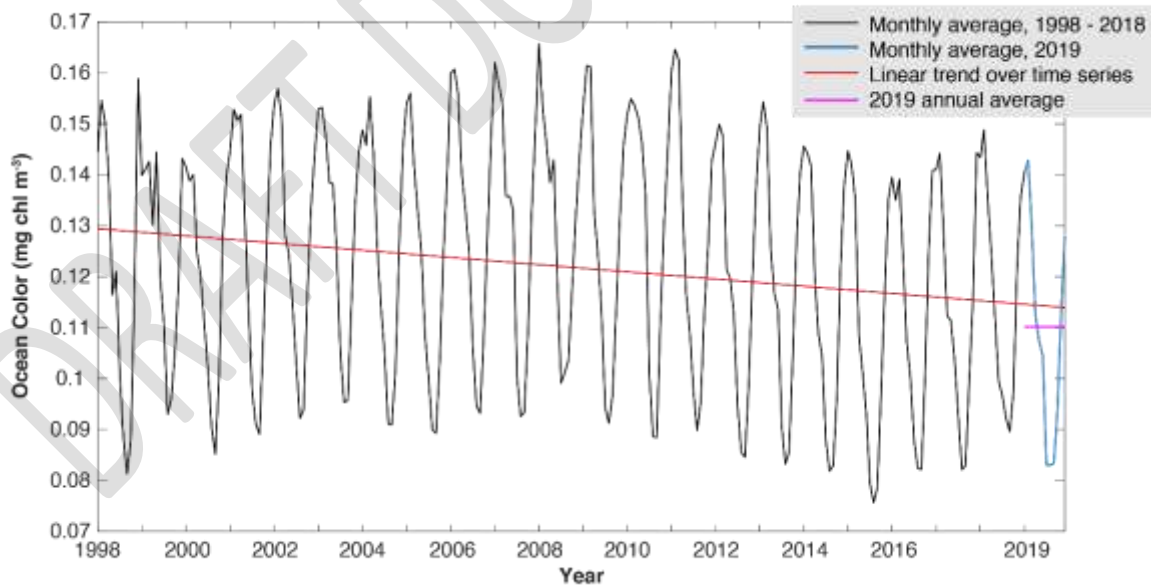


Figure 15 Time series of monthly average chlorophyll concentration over the longline fishing grounds outlined in Fig. 14.

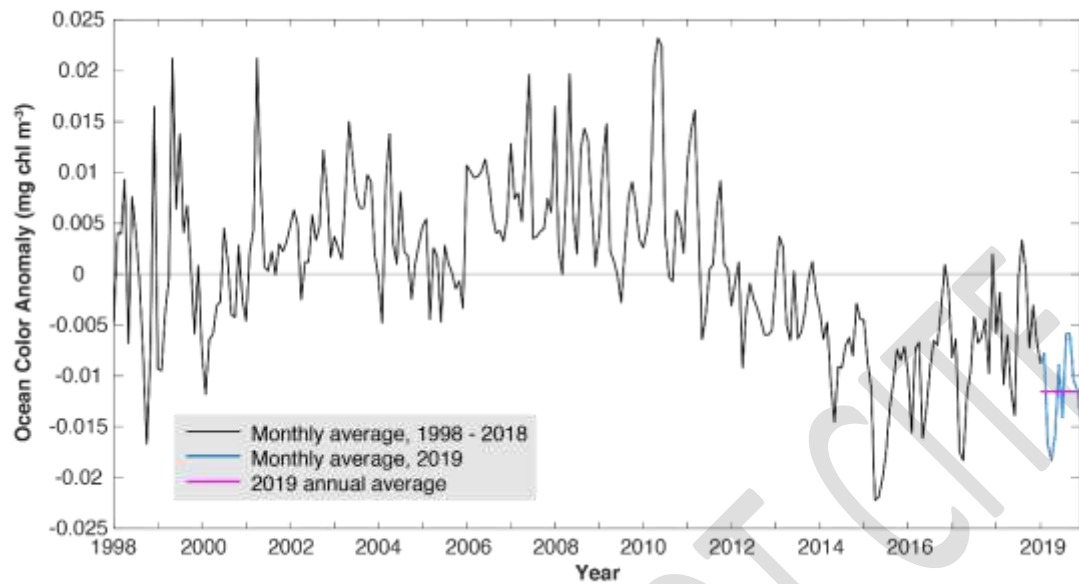


Figure 16 Time series of monthly average chlorophyll concentration anomaly over the longline fishing grounds outlined in Fig. 14.

Rationale: Phytoplankton are the foundational food source for the fishery. Changes in phytoplankton abundance have been linked to both natural climate variability and anthropogenic climate change. These changes have the potential to impact fish abundance, size, and catch.

Status: The mean monthly chlorophyll concentration was $0.11 \text{ mg chl m}^{-3}$ in 2019. Monthly mean chlorophyll concentrations ranged from $0.08 - 0.14 \text{ mg chl m}^{-3}$, within the range of values observed over the period of record ($0.0757 - 0.1657$). Over the period of record, monthly chlorophyll concentrations have declined by $0.016 \text{ mg chl m}^{-3}$. Chlorophyll concentrations across the region were fairly close to the climatological average in 2017, though some anomalies were observed at the far northern and southern boundaries of the longline fishing ground.

Description: Satellite remotely-sensed ocean color is used to determine chlorophyll concentrations in the pelagic surface ocean. These data can be used as a proxy for phytoplankton abundance. A time series of median monthly chlorophyll-a concentrations averaged over the Hawai`i longline region is presented. Additionally, spatial climatologies and anomalies are shown. European Space Agency (ESA) Climate Change Initiative (CCI) data are used for this indicator (Sathyendranath et al. 2018).

Timeframe: Monthly

Region/Location: Hawai`i longline region: $5^{\circ} - 45^{\circ}\text{N}$, $180^{\circ} - 120^{\circ}\text{W}$

Measurement Platform: Satellite

Sourced from: NOAA OceanWatch (2020).

1.1.2.11 NORTH PACIFIC SUBTROPICAL FRONT (STF) AND TRANSITION ZONE CHLOROPHYLL FRONT (TZCF)

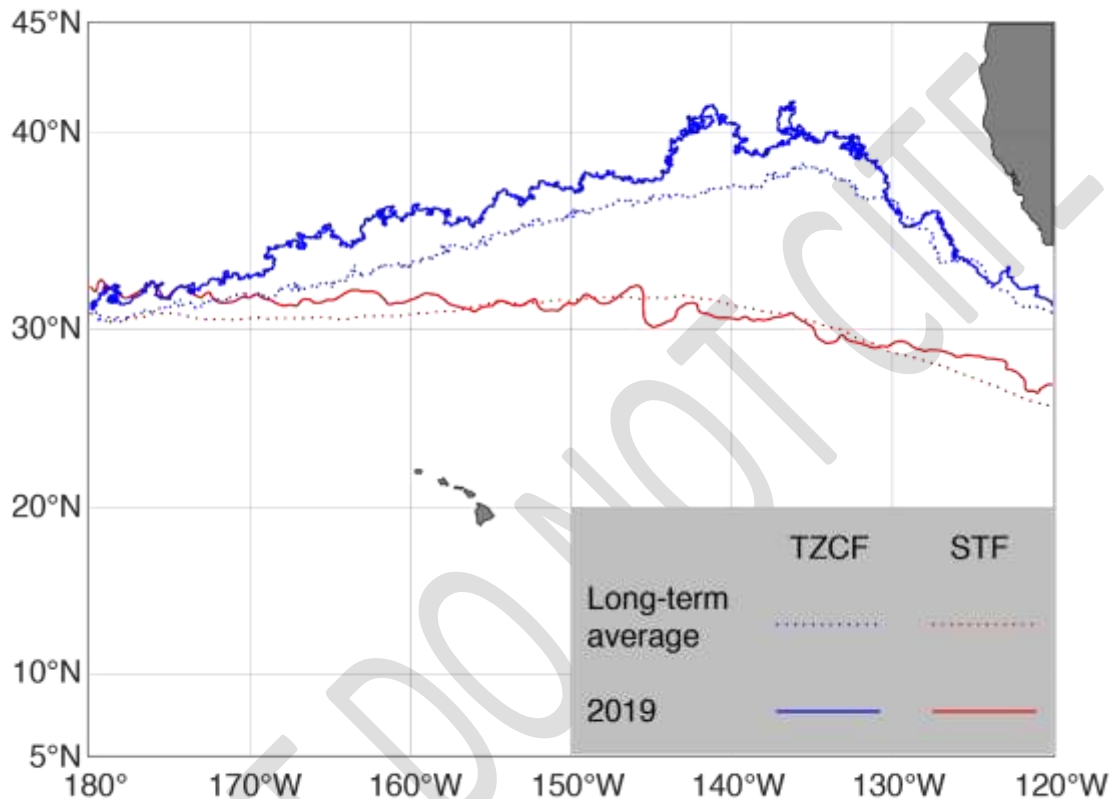


Figure 17 Average positions of the transition zone chlorophyll front (TZCF, blue lines) and subtropical front (STF, red lines) in 2019 (solid lines) and over a long-term average (dotted lines). The long-term average for the TZCF spans 1998 – 2018. The long-term average for the STF spans 1985 – 2018.

Rationale: The STF is targeted by the swordfish fishery. Additionally, both the STF and TZCF are used as migration and foraging corridors by both commercially-valuable and protected species. Northward displacement of the frontal zone can increase the distance fishing vessels must travel to set their gear. This can, in turn, increase operational expenses. The positions of the fronts vary in response to natural climate variations. Long-term northward displacement of the frontal zone may also result from anthropogenic climate change.

Status: During the first quarter of 2019, the STF was slightly north of average west of 160°W and east of 130°W, average from about 160 – 145°W, just south of average from 145 – 130°W. The TZCF was a few degrees north of average, particularly west of 130°W.

Description: The subtropical front (STF) is marked by the 18 °C sea surface temperature (SST) isotherm and the transition zone chlorophyll front (TZCF) by the 0.2 mg chl-a m⁻³ isopleth (Bograd *et al.* 2004; Polovina *et al.* 2001). They roughly mark the northern boundary of the North Pacific subtropical gyre as well as the northern extent of the Hawai`i-based longline fishery. Both fronts migrate in a meridional direction on a seasonal basis and their positions are impacted by the phase of the El Niño – Southern Oscillation (ENSO). Due to significant seasonal variation, the climatology and anomaly (2017) are presented for the first quarter of the year only. The STF is determined from CoralTemp data (see SST indicator) and the TZCF is determined from ESA CCI data (see ocean color indicator).

Timeframe: Annual, seasonal

Region: Hawai`i longline region: 5° – 45°N, 180° – 120°W

Measurement Platform: Satellite

Sourced from: Bograd *et al.* (2004), Polovina *et al.* (2001), and NOAA OceanWatch (2020).

1.1.2.12 ESTIMATED MEDIAN PHYTOPLANKTON SIZE

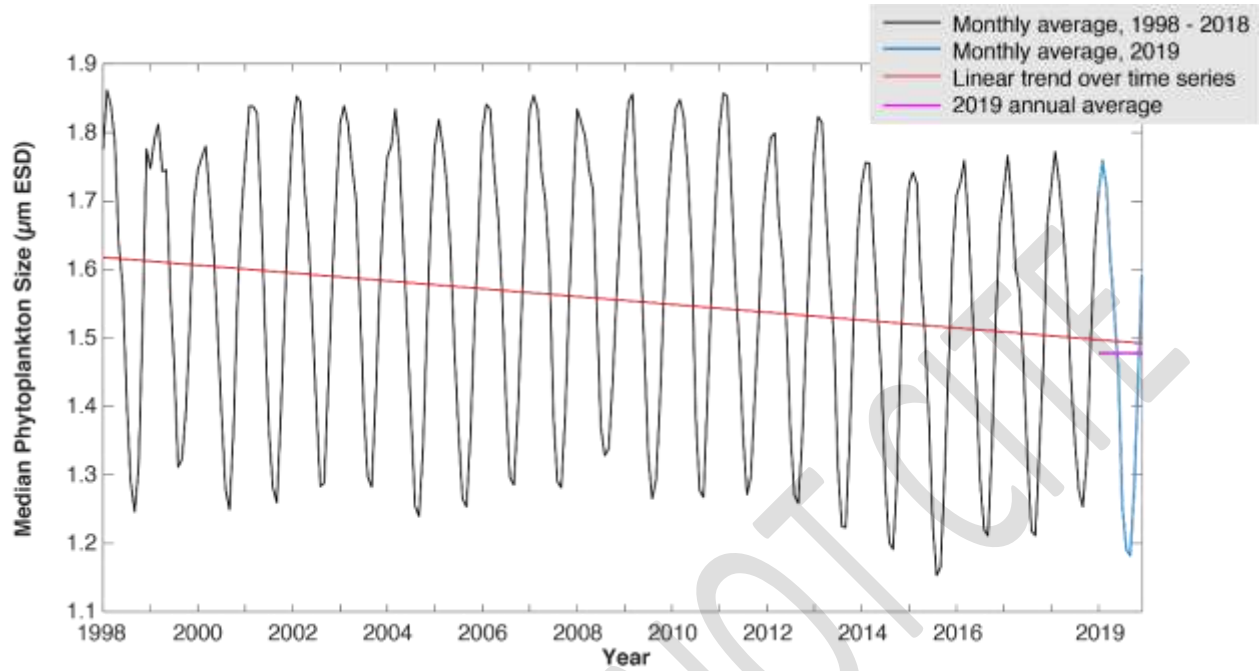


Figure 18 Time series of monthly median phytoplankton size over the longline fishing grounds outlined in Fig. 18

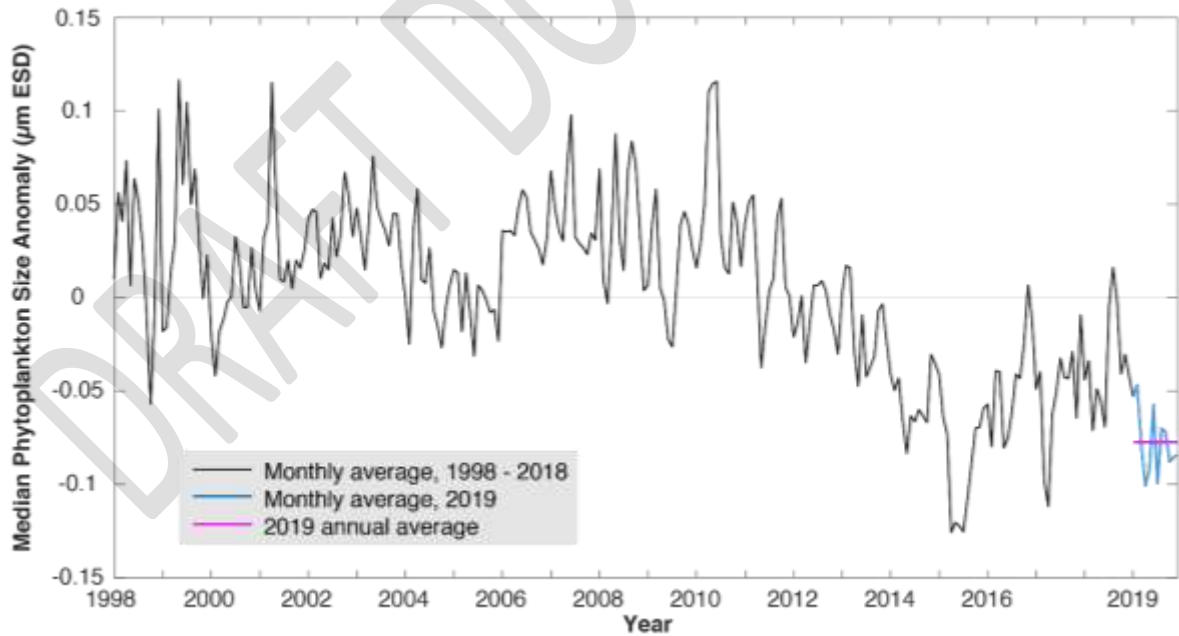


Figure 19 Time series of monthly median phytoplankton size anomaly over the longline fishing grounds outlined in Fig. 18.

Rationale: Phytoplankton are the base of the food web and their abundance influences the food available to all higher trophic levels from zooplankton through tunas. Some studies project that climate change will result in both fewer and smaller phytoplankton. This would reduce the food available to all members of the food web. Understanding trends in phytoplankton abundance and size structure, how they are influenced by oceanographic conditions, and how they influence tuna abundance and size structure are areas of active research.

Status: The mean monthly phytoplankton cell size was 1.48 μm Equivalent Spherical Diameter (ESD) in 2019. Monthly mean cell size ranged from 1.18 – 1.76 μm ESD during this period, within the range of values observed over the period of record (1.15 – 1.86 μm ESD). Over the period of record, median phytoplankton size has declined by 0.13 μm ESD.

Description: Median phytoplankton cell size can be estimated from satellite remotely sensed SST and ocean color (Barnes et al. 2011). A time series of monthly median phytoplankton cell size averaged over the Hawai`i longline region is presented. Additionally, spatial climatologies and anomalies are shown. NOAA CoralTemp (see SST indicator) and ESA OC-CCI data (see ocean color indicator) are used to calculate median phytoplankton cell size.

Timeframe: Monthly

Region: Hawai`i longline region: 15° – 45°N, 180° – 120°W

Measurement Platform: Satellite

Sourced from: NOAA OceanWatch (2020) and Barnes et al. (2011).

1.1.2.13 FISH COMMUNITY SIZE STRUCTURE

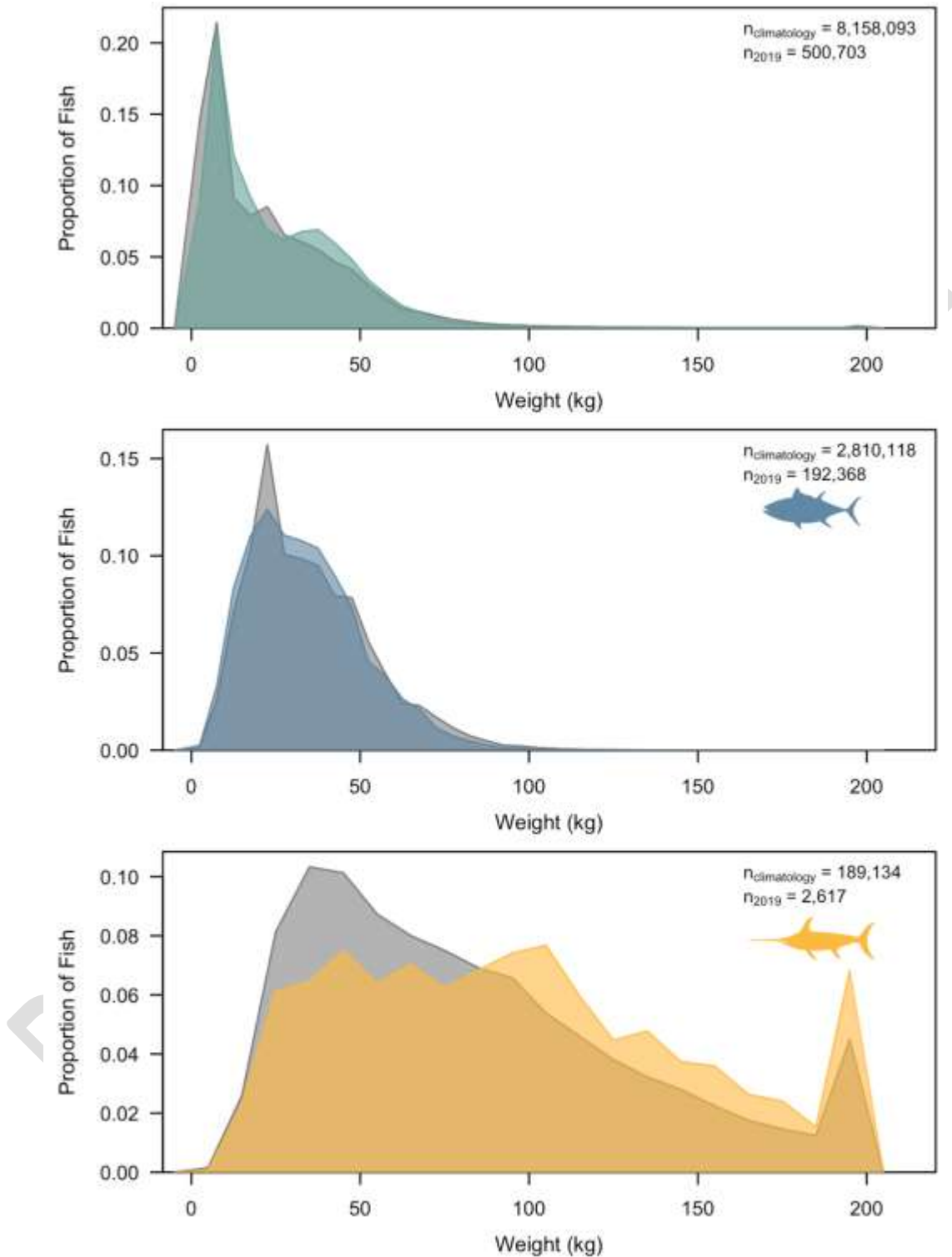


Figure 20 The climatological (2000 – 2018; grey) and 2019 (color) distribution of weights for all fish (top), bigeye tuna from deep sets (middle), and swordfish from shallow sets (bottom).

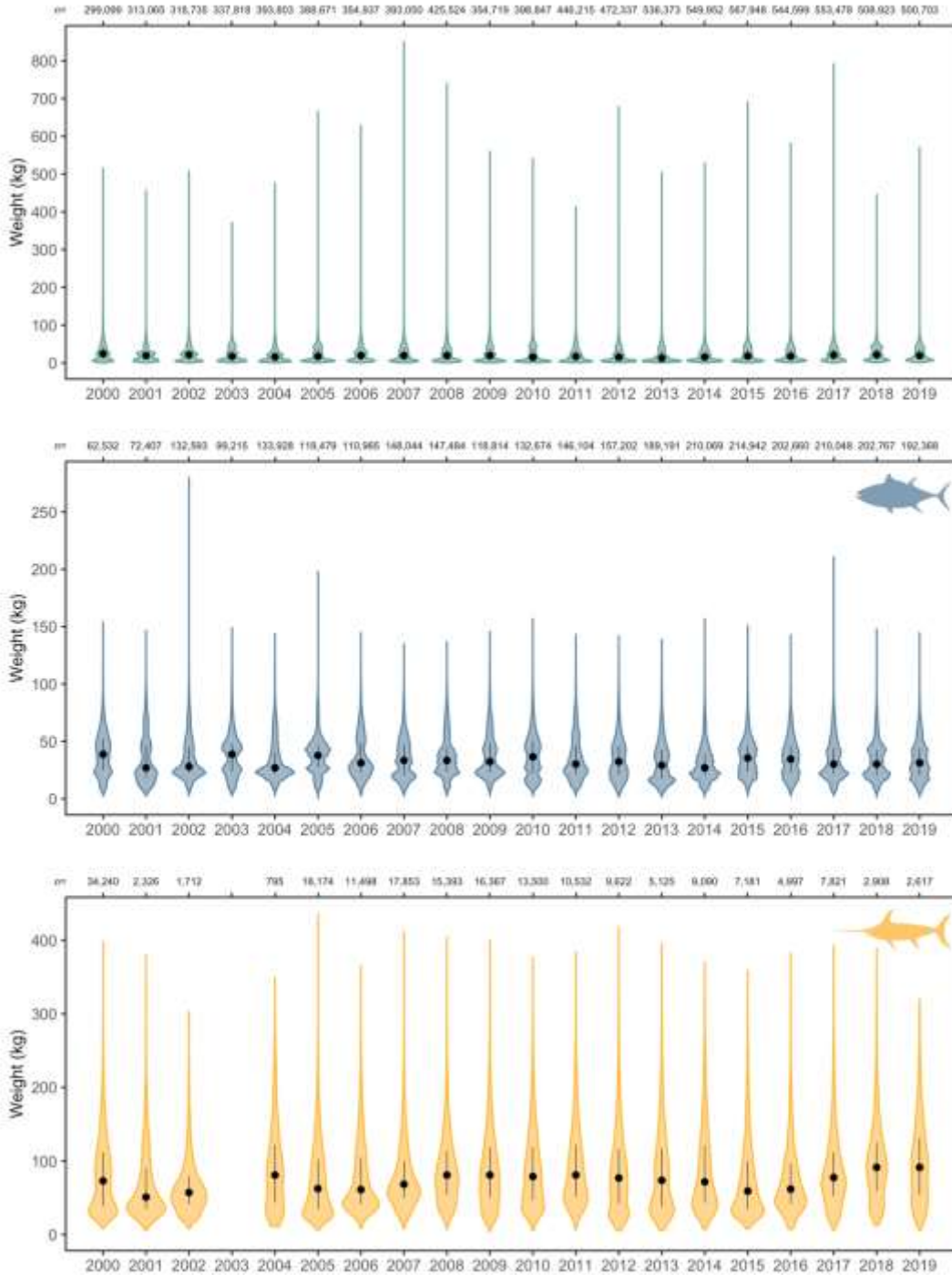


Figure 21 The annual distribution of weights of all fish (top), bigeye tuna from deep sets (middle), and swordfish from shallow sets (bottom), with circles denoting median weight, black lines showing the range of the middle 50% of fish, and width of shading proportional to the number of fish of a given weight.

Rationale: Fish size can be impacted by a number of factors, including climate. Currently, the degree to which the fishery’s target species are impacted by climate, and the scale at which these impacts may occur, is largely unknown. Ongoing collection of size structure data is necessary for detecting trends in community size structure and attributing causes of these trends.

Understanding trends in fish size structure and how oceanographic conditions influence these trends is an area of active research.

Status: For the longline fishery as a whole, fish were somewhat larger than usual in 2019 with a higher proportion of 40 – 50 kg fish. This peak may have been driven by an above average proportion of bigeye tuna in this size range. Swordfish also appeared larger than average in 2019, with an above average proportion of fish being 100 kg or larger.

In 2019, the median bigeye weight was 31.3 kg, and the median swordfish weight was 91.4 kg. The median fish weight for all species caught was 19.4 kg. The median weight of swordfish was at the maximum of the range of median weights seen across previous years, 50.9 – 91.4 kg. Median weights for all species and for bigeye were within the bounds observed over the time series from 2000 to 2018. There was no significant trend in bigeye, swordfish, or all species’ median weight over the full time series. However, the median weight of swordfish has increased steadily since 2015.

Description: The weight of individual fish moving through the Honolulu auction is available from 2000 through the present. Using these weights, community size structure is presented. A standardized pooled climatological distribution is presented, as is the 2019 distribution. Similar distributions for target species (bigeye tuna and swordfish) are also presented. Annual time series of pooled target species weights are presented as violin plots. Bigeye weights are from deep sets (≥ 15 hooks per float) only. Swordfish weights are from shallow sets (< 15 hooks per float) only. The Honolulu auction reports weights for gilled and gutted fish. A conversion factor is used to calculate the whole fish weights used for this indicator (Langley et al., 2006).

Timeframe: Annual.

Region: Hawai`i-based longline fishing grounds.

Measurement Platform: *In-situ* measurement.

Sourced from: Hawai`i Division of Aquatic Resources Measurement Platform and Langley et al. (2006).

1.1.2.14 BIGEYE WEIGHT-PER-UNIT-EFFORT

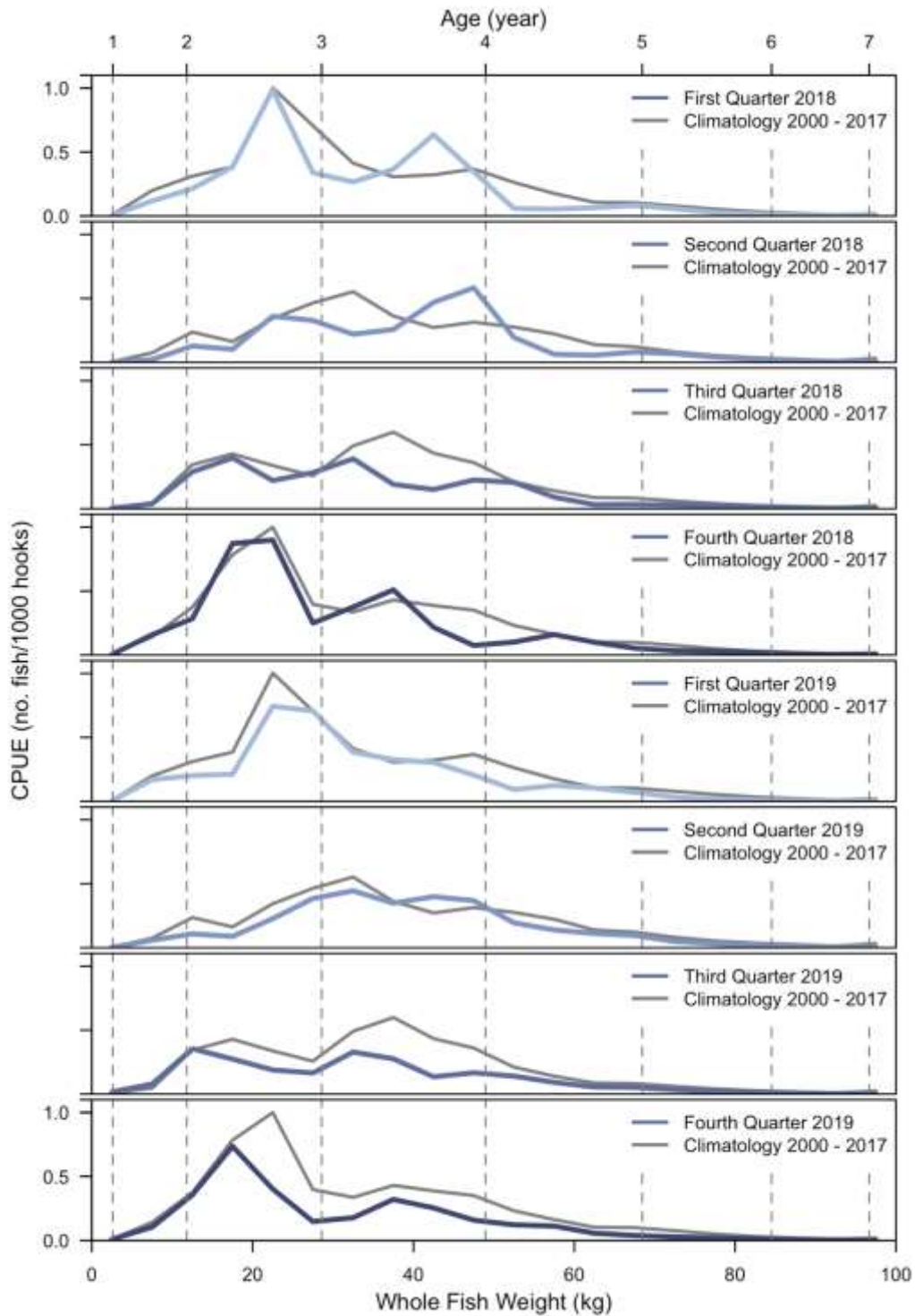


Figure 22 Quarterly deep-set bigeye tuna weight per unit effort for 2018 – 2019 (color) and the climatological average (2000 – 2017).

Rationale: Tracking the progression of growing size classes through time can provide a strong indication of recruitment pulses. The timing of these pulses is not yet well understood, particularly in terms of how they relate to climate impacts such as interannual variability. Improving this understanding could lead to the ability to project future yields and is an area of active research.

Status: No peak in the CPUE of two-year-old bigeye was observed in 2018 or 2019, suggesting there will not be a peak in the CPUE of four- and five-year old bigeye in 2020 to 2021.

Description: Quarterly time series of bigeye weight-per-unit-effort (hooks set) is presented for the previous two years. Fish weights are those of bigeye tuna received at the Honolulu auction. The Honolulu auction reports weights for gilled and gutted fish. A conversion factor is used to calculate the whole fish weights used for this indicator (Langley *et al.*, 2006). Note the quarterly (colored) and climatological (grey) distributions of bigeye tuna weight-per-unit-effort in Figure . Bigeye weights are from sets using ≥ 15 hooks per float.

Timeframe: Quarterly.

Region: Hawai`i-based longline fishing grounds.

Measurement Platform: *In-situ* measurement.

Sourced from: Hawai`i Division of Aquatic Resources.

1.1.2.15 BIGEYE RECRUITMENT INDEX

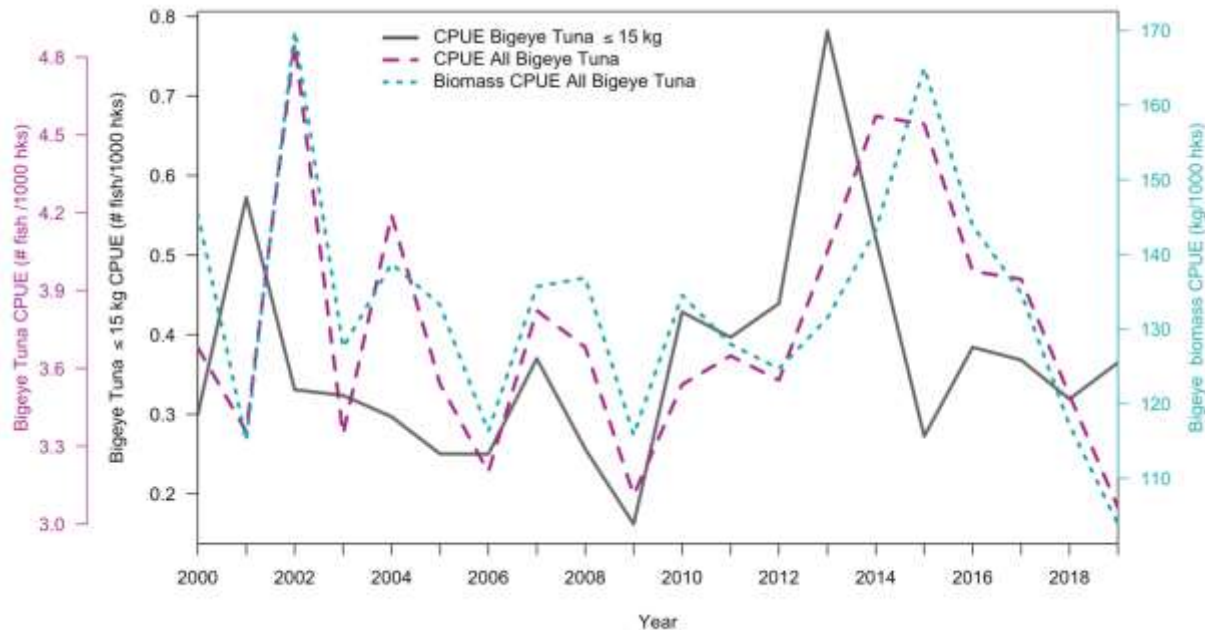


Figure 23 Annual CPUE of bigeye tuna ≤ 15 kg (grey solid line), CPUE of all bigeye tuna (pink dashed line), and biomass CPUE (blue dotted line) from 2000 – 2019, all from deep sets.

Rationale: Catch rates of small bigeye tuna (≤ 15 kg) peak two years prior to peaks in catch rates (CPUE) and biomass (weight-per-unit-effort), indicating a recruitment pulse and allowing for predictions regarding increases in total catch of the fishery. The timing of these pulses is not yet well understood, particularly in terms of how they relate to climate impacts such as interannual variability. Improving this understanding could lead to the ability to project future yields and is an area of active research.

Status: In 2019, the CPUE of bigeye ≤ 15 kg was 0.37 fish per 1,000 hooks set. This is within the range observed over the previous 19 years (0.16 – 0.79 fish per 1,000 hooks set) and at this time does not appear indicative of a strong recruitment pulse such as was seen in 2001 or 2013.

Description: Time series of small (≤ 15 kg) and total bigeye tuna catch-per-unit-effort (hooks set) and weight-per-unit-effort (hooks set) for all bigeye tuna is presented. Fish weights are those of bigeye tuna received at the Honolulu auction. The Honolulu auction reports weights for gilled and gutted fish. A conversion factor is used to calculate the whole fish weights used for this indicator (Langley et al. 2006).

Timeframe: Annual.

Region: Hawai`i-based longline fishing grounds.

Measurement Platform: Model-derived.

Sourced from: Hawai`i Division of Aquatic Resources and Langley et al. (2006).

1.1.2.16 BIGEYE TUNA CATCH RATE FORECAST

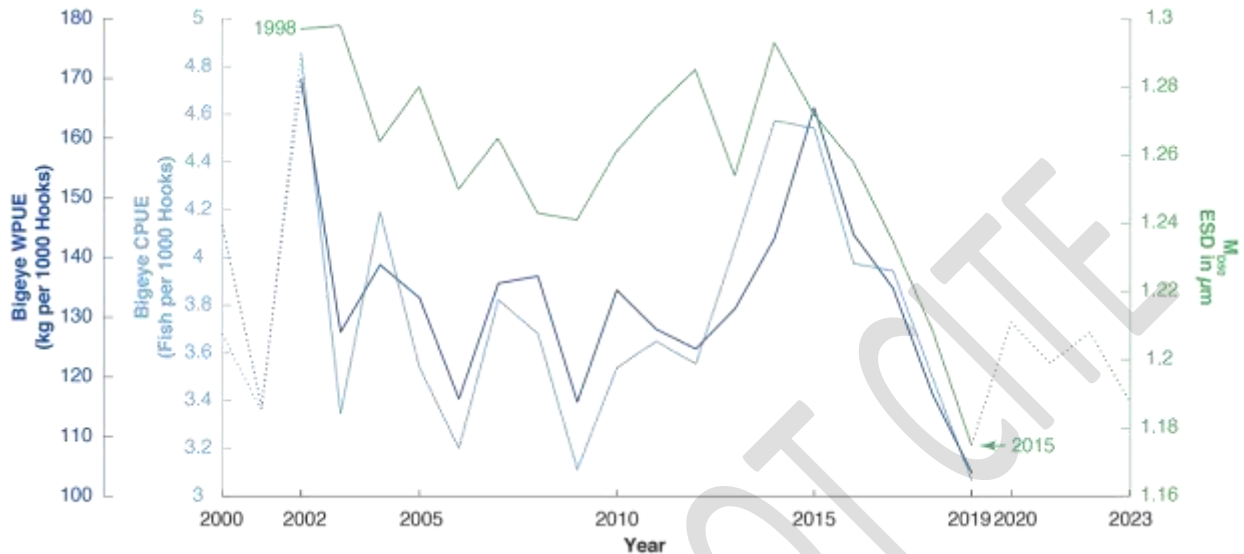


Figure 24 Annual WPUE (dark blue) and CPUE (light blue) of bigeye tuna from deep sets, as well as four-year lagged median phytoplankton size (M_{D50} , green). Dashed lines indicate years that are outside the forecast period described in the text.

Rationale: Recent work has shown that average phytoplankton size can be used to predict bigeye tuna catch rates four years in advance (Woodworth-Jefcoats and Wren, In Review). The hypothesized mechanism behind this relationship is that larger phytoplankton are indicative of higher quality food for the zooplankton upon which larval and juvenile bigeye tuna prey. With higher quality prey available, more bigeye tuna survive into adulthood and recruit to the fishery.

Status: In 2019, the median size of phytoplankton across the Hawaii longline fishing grounds was 1.19 µm Equivalent Spherical Diameter (ESD). This is within the range observed over the previous 21 years (1.18 – 1.30 µm ESD). Median phytoplankton sizes from 2016 – 2019 suggest that bigeye catch rates may increase slightly over the next four years, though will likely not increase to the catch rates seen in 2002 or 2015.

Description: Time series of median phytoplankton, total bigeye tuna catch-per-unit-effort (hooks set) and weight-per-unit-effort (hooks set) for all bigeye tuna are presented. Median phytoplankton size is derived from satellite remotely sensed sea surface and ocean color data (see indicator above). Fish weights are those of bigeye tuna received at the Honolulu auction. The Honolulu auction reports weights for gilled and gutted fish. A conversion factor is used to calculate the whole fish weights used for this indicator (Langley et al. 2006).

Timeframe: Annual.

Region: Hawai`i-based longline fishing grounds (0° – 40°N, 180° – 150°W and 15° – 36°N, 150° – 125°W).

Measurement Platform: Model-derived from satellite remotely sensed data.

Sourced from: NOAA OceanWatch (2020), Hawai'i Division of Aquatic Resources, and Langley et al. (2006).

1.1.3 BACKGROUND AND RATIONALE FOR INDICATORS

The reasons for the Council's decision to provide and maintain an evolving discussion of climate conditions as an integral and continuous consideration in their deliberations, decisions, and reports are numerous:

- Emerging scientific and community understanding of the impacts of changing climate conditions on fishery resources, the ecosystems that sustain those resources, and the communities that depend upon them;
- Recent Federal Directives including the 2010 implementation of a National Ocean Policy that identified Resiliency and Adaptation to Climate Change and Ocean Acidification as one of nine National priorities as well as the development of a Climate Science Strategy by NMFS in 2015 and the subsequent development of the Pacific Islands Regional Action Plan for climate science; and
- The Council's own engagement with NOAA as well as jurisdictional fishery management agencies in American Samoa, CNMI, Guam, and Hawai'i as well as fishing industry representatives and local communities in those jurisdictions.

In 2013, the Council began restructuring its Marine Protected Area/Coastal and Marine Spatial Planning Committee to include a focus on climate change, and the committee was renamed as the Marine Planning and Climate Change (MPCC) Committee. In 2015, based on recommendations from the committee, the Council adopted its Marine Planning and Climate Change Policy and Action Plan, which provided guidance to the Council on implementing climate change measures, including climate change research and data needs. The revised Pelagic Fisheries Ecosystem Plan (FEP; February 2016) included a discussion on climate change data and research as well as a new objective (Objective 9) that states the Council should consider the implications of climate change in decision-making, with the following sub-objectives:

- 4 To identify and prioritize research that examines the effects of climate change on Council-managed fisheries and fishing communities.
- 5 To ensure climate change considerations are incorporated into the analysis of management alternatives.
- 6 To monitor climate change related variables via the Council's Annual Reports.
- 7 To engage in climate change outreach with U.S. Pacific Islands communities.

Beginning with the 2015 report, the Council and its partners began providing continuing descriptions of changes in a series of climate and oceanic indicators.

This annual report focuses previous years' efforts by refining existing indicators and improving communication of their relevance and status. Future reports will include additional indicators as the information becomes available and their relevance to the development, evaluation, and

revision of the FEPs becomes clearer. Working with national and jurisdictional partners, the Council will make all datasets used in the preparation of this and future reports available and easily accessible.

1.1.4 RESPONSE TO PREVIOUS COUNCIL RECOMMENDATIONS

There were no Council recommendations relevant to the climate and oceanic indicators section of the annual SAFE report in 2019.

At its 170th meeting from June 20-22, 2017, the Council directed staff to support the development of community training and outreach materials and activities on climate change. In addition, the Council directed staff to coordinate a “train-the-trainers” workshop that includes NOAA scientists who presented at the 6th Marine Planning and Climate Change Committee (MPCCC) meeting and the MPCCC committee members in preparation for community workshops on climate and fisheries. The Council and NOAA partnered to deliver the workshops in the fall of 2017 to the MPCCC members in Hawaii (with the Hawaii Regional Ecosystem Advisory Committee), as well as American Samoa, Guam, and the CNMI (with their respective Advisory Panel groups). Feedback from workshop participants has been incorporated into this year’s climate and oceanic indicator section. To prepare for community outreach, Guam-based MPCCC members conducted a climate change survey and shared the results with the MPCCC at its 7th meeting on April 10th and 11th, 2018. The Council also directed staff to explore funding avenues to support the development of additional oceanic and climate indicators, such as wind and extratropical storms. These indicators were added to this module by corresponding Plan Team members in 2018.

Prior to holding its 8th meeting, the MPCCC was disbanded in early 2019, re-allocating its responsibilities among its members already on other committees or teams, such as the Fishery Ecosystem Plan Teams.

1.1.5 CONCEPTUAL MODEL

In developing this chapter, the Council relied on a number of recent reports conducted in the context of the U.S. National Climate Assessment including, most notably, the 2012 Pacific Islands Regional Climate Assessment and the Ocean and Coasts chapter of the 2014 report on a Pilot Indicator System prepared by the National Climate Assessment and Development Advisory Committee (NCADAC).

The Advisory Committee Report presented a possible conceptual framework designed to illustrate how climate factors can connect to and interact with other ecosystem components to impact ocean and coastal ecosystems and human communities. The Council adapted this model with considerations relevant to the fishery resources of the Western Pacific Region:

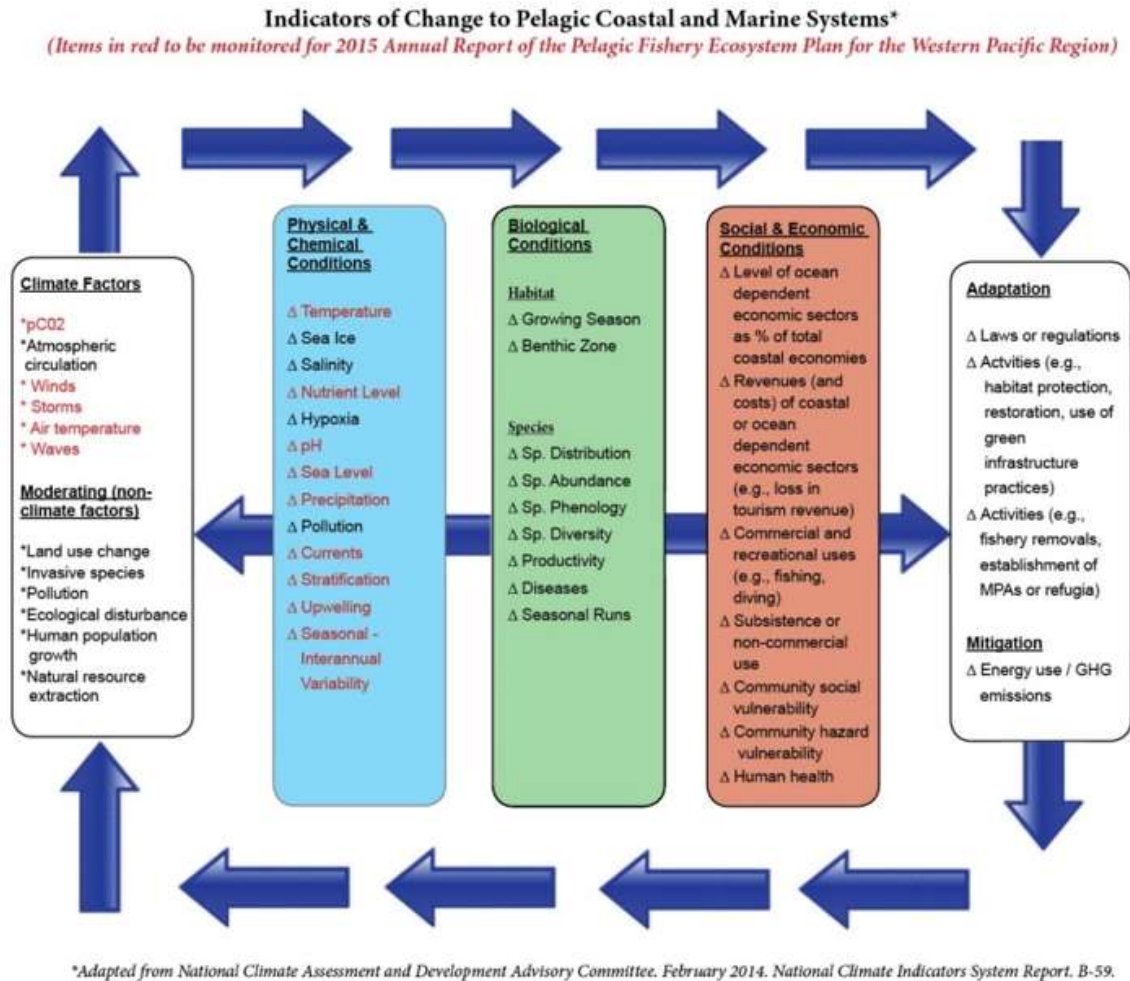


Figure 163. Indicators of change of pelagic coastal and marine systems; conceptual model

As described in the 2014 NCADAC report, the conceptual model presents a “simplified representation of climate and non-climate stressors in coastal and marine ecosystems.” For the purposes of this Annual Report, the modified Conceptual Model allows the Council and its partners to identify indicators of interest to be monitored on a continuing basis in coming years. The indicators shown in red were considered for inclusion in the Annual SAFE Reports, though the final list of indicators varied somewhat. Other indicators will be added over time as data become available and an understanding of the causal chain from stressors to impacts emerges.

The Council also hopes that this Conceptual Model can provide a guide for future monitoring and research. This guide will ideally enable the Council and its partners to move forward from observations and correlations to understanding the specific nature of interactions, and to develop capabilities to predict future changes of importance in the developing, evaluating, and adapting of FEPs in the Western Pacific region.s

1.1.6 OBSERVATIONAL AND RESEARCH NEEDS

Through preparation of this and previous Annual Pelagic Reports, the Council has identified a number of observational and research needs that, if addressed, would improve the information content of future Climate and Oceanic Indicators section. This information would provide fishery managers, the fishing industry, and community stakeholders with better understanding and predictive capacity that is vital to sustaining a resilient and vibrant fishery in the Western Pacific. These observational and research needs are to:

- Emphasize the importance of continuing the climate and ocean indicators used in this report so that a consistent, long-term record can be maintained and interpreted;
- Develop agreements among stakeholders and research partners to ensure the sustainability, availability, and accessibility of climate and ocean indicators, associated datasets, and analytical methods used in this and future reports;
- Improve monitoring and understanding of the impacts of changes in ocean temperature, pH and ocean acidity, ocean oxygen content and hypoxia, and sea level rise through active collaboration by all fishery stakeholders and research partners;
- Develop, test, and provide access to additional climate and ocean indicators that can improve the Pelagic Conceptual Model;
- Investigate the connections between climate variables and other indicators in the Pelagic Conceptual Model to improve understanding of changes in physical, chemical, biological, and socio-economic processes and their interactions in the regional ecosystem;
- Develop predictive models that can be used for scenario planning to account for unexpected changes and uncertainties in the regional ecosystem and fisheries;
- Foster applied research in ecosystem modeling to better describe current conditions and to better anticipate the future under alternative projections of climate and ocean change including changes in expected human benefits and their variability;
- Improve understanding of the connections between the Pacific Decadal Oscillation (PDO) and fisheries ecosystems beyond the North Pacific;
- Improve understanding of mahimahi and swordfish size in relation to the location and orientation of the transition zone chlorophyll front (TZCF);
- Explore the connections between sea surface conditions, stratification, and mixing;
- Identify the biological implications of tropical cyclones;
- Research cultural knowledge and practices for adapting to past climate changes and investigate how they might contribute to future climate adaptation; and
- Explore additional and/or alternative climate and ocean indicators that may have important effects of pelagic fisheries systems including:
 - Ocean currents and anomalies;
 - Eddy kinetic energy (EKE);
 - Near-surface wind velocity and anomalies;
 - Wave forcing and anomalies;
 - Oceanic nutrient concentration;
 - South Pacific convergence zones targeted by swordfish;
 - Standardized fish community size structure data for gear types, including the troll fishery for yellowfin and blue marlin;

- Additional estimates of phytoplankton abundance and size from satellite remotely-sensed sea surface temperature (SST) and ocean color measurements;
- Additional spatial coverage for the international purse seine fishery and the American Samoa longline fishery;
- Time series of species richness and diversity from catch data which could potentially provide insight into how the ecosystem is responding to physical climate influences; and
- Socio-economic indicators of effects of a changing climate on fishing communities and businesses

1.1.7 REFERENCES

- Barnes, C., Irigoien, X., De Oliveira, J.A.A., Maxwell, D., and S. Jennings, 2011. Predicting marine phytoplankton community size structure from empirical relationships with remotely sensed variables. *Journal of Plankton Research*, 33(1), pp. 13-24. doi: 10.1093/plankt/fbq088
- Bograd, S.J., Foley, D.G., Schwing, F.B., Wilson, C., Laurs, R.M., Polovina, J.J., Howell, E.A., and R.E. Brainard, 2004. On the seasonal and interannual migrations of the transition zone chlorophyll front. *Geophysical Research Letters*, 31, L17204. doi: 10.1029/2004GL020637.
- Fabry, V.J., Seibel, B.A., Feely, R.A., and J.C. Orr, 2008. Impacts of ocean acidification on marine fauna and ecosystem processes. *ICES Journal of Marine Science*, 65(3), pp. 414-432.
- Feely, R.A., Alin, S.R., Carter, B., Bednarsek, N., Hales, B., Chan, F., Hill, T.M., Gaylord, B., Sanford, E., Byrne, R.H., Sabine, C.L., Greeley, D., and L. Juranek, 2016. Chemical and biological impacts of ocean acidification along the west coast of North America. *Estuarine, Coastal and Shelf Science*, 183, pp. 260-270. doi: 10.1016/j.ecss.2016.08.04.
- HOT, 2020. Hawaii Ocean Time Series. School of Ocean and Earth Science and Technology, University of Hawaii Manoa. Accessed from <http://hahana.soest.hawaii.edu/hot/>.
- Howell, E.A., Hawn, D.R., and J.J. Polovina, 2010. Spatiotemporal variability in bigeye tuna (*Thunnus obesus*) dive behavior in the central North Pacific Ocean. *Progress in Oceanography*, 86, pp. 81-93. doi: 10.1016/j.pocean.2010.04.013.
- Karl, D.M. and R. Lukas, 1996. The Hawaii Ocean Time-series (HOT) program: Background, rationale and field implementation. *Deep Sea Research Part II: Topical Studies in Oceanography*, 43(2-3), pp.129-156.
- Keeling, C.D., Bacastow, R.B., Bainbridge, A.E., Ekdahl, C.A., Guenther, P.R., and L.S. Waterman, 1976. Atmospheric carbon dioxide variations at Mauna Loa Observatory, Hawaii. *Tellus*, 28(6), pp. 538-551.

- Knapp, K.R., Kruk, M.C., Levinson, D.H., Diamond, H.J., and C.J. Neumann, 2010. The International Best Track Archive for Climate Stewardship (IBTrACS): Unifying tropical cyclone best track data. *Bulletin of the American Meteorological Society*, 91, pp. 363-376. [doi:10.1175/2009BAMS2755.1](https://doi.org/10.1175/2009BAMS2755.1).
- Knapp, K. R., H. J. Diamond, J. P. Kossin, M. C. Kruk, C. J. Schreck, 2018: International Best Track Archive for Climate Stewardship (IBTrACS) Project, Version 4. NOAA National Centers for Environmental Information. <https://doi.org/10.25921/82ty-9e16>
- Langley, A., Okamoto, H., Williams, P., Miyabe, N., Bigelow, K., 2006. A summary of the data available for the estimation of conversion factors (processed to whole fish weights) for yellowfin and bigeye tuna. ME IP-3, WCPFC-SC2, Manila, Philippines, 7, 18 pp.
- NOAA Climate.gov, 2016. El Niño and La Niña: Frequently asked questions. Authored 18 January 2016. Accessed from <https://www.climate.gov/news-features/understanding-climate/el-ni%C3%B1o-and-la-ni%C3%B1a-frequently-asked-questions>.
- NOAA Climate Prediction Center (CPC), 2020. Oceanic Nino Index. Accessed from <https://www.cpc.ncep.noaa.gov/data/indices/oni.ascii.txt>
- NOAA ESRL, 2020a. Climate Indices: Monthly Atmospheric and Oceanic Time-Series. Earth System Research Laboratory, Physical Sciences Division. Accessed from <https://www.esrl.noaa.gov/psd/data/correlation/pdo.data>
- NOAA ESRL, 2020b. Full Mauna Loa CO₂ Record. Trends in Atmospheric Carbon Dioxide. Earth System Research Laboratory, Global Monitoring Division. Accessed from <https://www.esrl.noaa.gov/gmd/ccgg/trends/full.html>.
- NOAA ESRL, 2020c. NCEP Global Ocean Data Assimilation System (GODAS). Earth System Research Laboratory, Physical Sciences Division. Accessed from <https://www.esrl.noaa.gov/psd/data/gridded/data.godas.html>.
- NOAA OceanWatch, 2020. Conditions in the Hawaii longline fishing ground. OceanWatch Central Pacific Node. Accessed from <http://oceanwatch.pifsc.noaa.gov/indicators-longline.html>.
- Polovina, J.J., Howell, E.A., Kobayashi, D.R., and M.E. Seki, 2001. The transition zone chlorophyll front, a dynamic global feature defining migration and forage habitat for marine resources. *Progress in Oceanography*, 49, pp. 469-483.
- Sathyendranath S, Grant M, Brewin R.J.W, Brockmann C, Brotas V, Chuprin A, Doerffer R, Dowell M, Farman A, Groom S, Jackson T, Krasemann H, Lavender S, Martinez Vicente V, Mazeran C, Mélin F, Moore TS, Müller D, Platt T, Regner P, Roy S, Steinmetz F, Swinton J, Valente A, Zühlke M, Antoine D, Arnone R, Balch W.M, Barker K, Barlow R, Bélanger S, Berthon J-F, Beşiktepe Ş, Brando VE, Canuti E, Chavez F, Claustre H, Crout R, Feldman G, Franz B, Frouin R, García-Soto C, Gibb SW, Gould R, Hooker S,

Kahru M, Klein H, Kratzer S, Loisel H, McKee D, Mitchell BG, Moisan T, Muller-Karger F, O'Dowd L, Ondrusek M, Poulton AJ, Repecaud M, Smyth T, Sosik H.M, Taberner M, Twardowski M, Voss K, Werdell J, Wernand M, Zibordi G. (2018): ESA Ocean Colour Climate Change Initiative (Ocean_Colour_cci): Version 3.1 Data. Centre for Environmental Data Analysis *04 July 2018*.

doi:10.5285/9c334fbe6d424a708cf3c4cf0c6a53f5.

<http://dx.doi.org/10.5285/9c334fbe6d424a708cf3c4cf0c6a53f5>

Thoning, K.W., Tans, P.P., and W.D. Komhyr, 1989. Atmospheric carbon dioxide at Mauna Loa Observatory 2. Analysis of the NOAA GMCC data, 1974-1985. *Journal of Geophysical Research*, 94(D6), pp. 8549-8565.

Woodworth-Jefcoats, P.A., and J.L.K. Wren, 2020. Towards an environmental predictor of tuna recruitment. In Review.